AD-A095 595 IIT RESEARCH INST CHICAGO IL F/G 11/4
PHOTOELASTIC STUDIES OF INTERNAL STRESS DISTRIBUTIONS OF UNIDIR--ETC(U)
DEC 80 I M DANIEL, G M KOLLER, T NIIRO DAAG46-79-C-0083
UNCLASSIFIED IITR-M6062 AMMRC-TR-80-56 NL

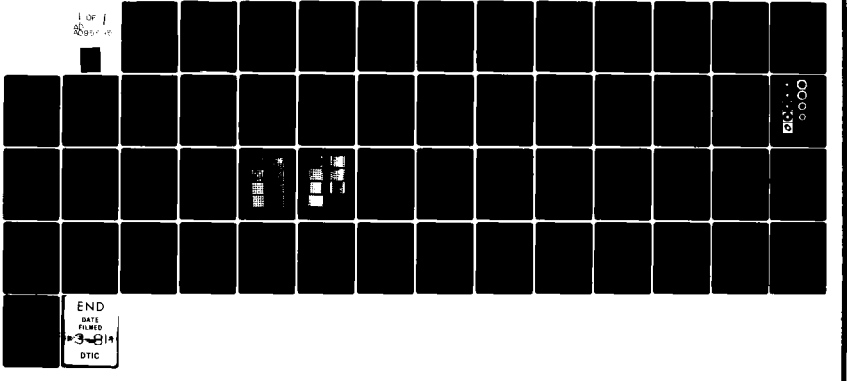

END
DATE FILMED
3-81
DTIC

AD A095555

(12)

AD

AMMRC TR 80-56

PHOTOELASTIC STUDIES OF INTERNAL STRESS DISTRIBUTIONS OF UNIDIRECTIONAL COMPOSITES

DECEMBER 1980

PREPARED BY

I. M. DANIEL
G. M. KOLLER
T. NIIRO

IIT RESEARCH INSTITUTE
10 WEST 35TH STREET
CHICAGO, IL 60616

FINAL REPORT CONTRACT NO. DAAG-46-79-C-0083

A

Prepared for

ARMY MATERIALS AND MECHANICS RESEARCH CENTER
Watertown, Massachusetts 02172

The findings in this report are not to be construed as an official Department of the Army position, unless so designated by other authorized documents.

Mention of any trade names or manufacturers in this report shall not be construed as advertising nor as an official indorsement or approval of such products or companies by the United States Government.

DISPOSITION INSTRUCTIONS

Destroy this report when it is no longer needed.
Do not return it to the originator.

UNCLASSIFIED

SECURITY CLASSIFICATION OF THIS PAGE (When Data Entered)

(19) REPORT DOCUMENTATION PAGE	READ INSTRUCTIONS BEFORE COMPLETING FORM
(18) 1. REPORT NUMBER: AMMRC TR-80-56 ✓	2. GOVT ACCESSION NO.: AD-A093 595
	3. RECIPIENT'S CATALOG NUMBER
4. TITLE (and Subtitle): PHOTOELASTIC STUDIES OF INTERNAL STRESS DISTRIBUTIONS OF UNIDIRECTIONAL COMPOSITES.	5. TYPE OF REPORT & PERIOD COVERED: (9) Final Report, 11 Sep 79 to 11 Sep 80
	6. PERFORMING ORG. REPORT NUMBER: (14) IITRI-M6062 ✓
7. AUTHOR(s): (17) I. M. Daniel, G. M. Koller, and T. Niiro	8. CONTRACT OR GRANT NUMBER(s): (15) DAAG46-79-C-0083
9. PERFORMING ORGANIZATION NAME AND ADDRESS: IIT Research Institute ✓, 10 West 35th Street, Chicago, Illinois 60616	10. PROGRAM ELEMENT, PROJECT, TASK AREA & WORK UNIT NUMBERS: (16) D/A Project: 1L161102AH42, AMCMS Code: 61102.11.H42, Agency Accession: DA OG0776
11. CONTROLLING OFFICE NAME AND ADDRESS: Army Materials and Mechanics Research Center, ATTN: DRXMR-AP, Watertown, Massachusetts 02172 (12)	12. REPORT DATE: (11) December 1980
	13. NUMBER OF PAGES: 42
14. MONITORING AGENCY NAME & ADDRESS (if different from Controlling Office)	15. SECURITY CLASS. (of this report): Unclassified
	15a. DECLASSIFICATION/DOWNGRADING SCHEDULE

16. DISTRIBUTION STATEMENT (of this Report)

Approved for public release; distribution unlimited.

17. DISTRIBUTION STATEMENT (of the abstract entered in Block 20, if different from Report)

18. SUPPLEMENTARY NOTES

Presented at the Army Composite Materials Research Review, Williamstown, Massachusetts, 29-31 October 1980.

19. KEY WORDS (Continue on reverse side if necessary and identify by block number)

Composites	Stress analysis
Plastics	Failure criteria
Photoelasticity	Tensile strength

20. ABSTRACT (Continue on reverse side if necessary and identify by block number)

Two-dimensional photoelastic models were used to determine internal loading- and residual-stress distributions on the transverse cross section of unidirectional composites. The variation of residual stress was determined as a function of post-curing temperature for a room-temperature cured matrix resin. Maximum stresses and strains were determined in the matrix of a unidirectional composite with a 0.50 fiber volume ratio. Prototype composite specimens were made with the same matrix material and the same

DD FORM 1 JAN 73 1473 EDITION OF 1 NOV 65 IS OBSOLETE

UNCLASSIFIED

SECURITY CLASSIFICATION OF THIS PAGE (When Data Entered)

Block No. 20

fiber volume ratio and were cured under the same conditions as the models. The transverse strength of these prototype specimens was predicted satisfactorily from results of model tests for the room-temperature cured specimens. In the case of the post-cured specimens, the predictions were higher than the measured strength.

FOREWORD

This is the Final Report on IIT Research Institute Project No. M6062, "Photoelastic Studies of Internal Stress Distributions of Unidirectional Composites," prepared by IITRI for the Army Materials and Mechanics Research Center, under Contract No. DAAG46-79-C-0083. The work described herein was conducted in the period 11 September 1979 to 11 September 1980. Dr. A. F. Wilde is the Contracting Officer's Technical Representative. IIT Research Institute personnel who made contributions to the work reported herein include Dr. I. M. Daniel and Messrs. G. M. Koller, W. G. Hamilton and T. Niiro.

Respectfully submitted,
IIT RESEARCH INSTITUTE

I. M. Daniel
Science Advisor
Materials Technology Division

APPROVED:

S. A. Bortz
Senior Engineering Advisor
Materials Technology Division

TABLE OF CONTENTS

LIST OF FIGURES

LIST OF FIGURES (CONT'D)

PHOTOELASTIC STUDIES OF INTERNAL STRESS DISTRIBUTIONS OF UNIDIRECTIONAL COMPOSITES

1. INTRODUCTION

The behavior of composite structures subject to loading and environmental fluctuations is intimately related to the micromechanics of load transfer between the constituent parts of the composite, i.e., fiber and matrix.

Matrix stresses on a transverse plane of unidirectional composite arise due to matrix shrinkage during curing, differential thermal expansion, moisture absorption and external loading. For relatively low fiber volume ratios, resin shrinkage produces compressive radial stresses and longitudinal shear stresses around the fibers in the matrix. The fibers themselves are subjected to radial and longitudinal compression. Shrinkage stresses are usually studied by means of two-dimensional photoelastic models of the transverse cross section of the composite.

The state of residual stress around fibers is greatly affected by the environment, i.e., temperature and moisture. A uniform temperature change throughout the composite is exactly equivalent to the effect of matrix shrinkage. A uniform temperature increase may nullify any beneficial effects that the radial compressive shrinkage stresses may have. A similar situation exists when a uniform moisture absorption occurs. This tends to relieve the curing residual stresses and thus decrease the transverse tensile strength.

A great deal of analytical work has been reported on the micromechanics of unidirectional composites.[1-22] Related experimental work has consisted primarily of two-dimensional photoelastic studies. Shrinkage stresses around inclusions have been studied by Daniel and Durelli[23,24] and Koufopoulos and Theocaris[25] by means of two-dimensional models. The effects of external loading were studied by Sampson[26] and Daniel.[27,28] An extensive three-dimensional study of the effects of shrinkage and external

loading was conducted by Marloff and Daniel using a realistic three-dimensional fiber-reinforced composite model.[29]

Transverse tensile loading of a unidirectional composite results in high strain concentrations in the matrix. In this case the matrix stresses and strains are the governing criteria of failure. The transverse tensile behavior of unidirectional composites is greatly influenced by the residual stresses produced by matrix shrinkage, by temperature and moisture absorption. The extent to which these parameters influence the behavior of the composite is very important and merits more careful experimental investigation.

This report describes an experimental investigation using models and prototype composite specimens to determine internal residual and loading stress distributions and correlate them with the transverse tensile strength of unidirectional composites.

2. SPECIMEN PREPARATION

Model composite specimens simulating the transverse cross-section of unidirectional composites were prepared by casting epoxy around an array of glass disks. The glass disks were 1.27 cm (0.5 in.) in diameter arranged in a square array with a clear spacing corresponding to a fiber volume ratio of $V_f = 0.50 \pm 0.02$ as shown in Fig. 1. A single isolated disk was also included in the same specimen for reference.

The matrix material used was Dow Epoxy Resin (DER 332) cured with twelve percent by weight of Dow Epoxy Hardener (DEH 24, Diethylene Tetramine). The resin was mixed with the hardener and deaerated in a vacuum jar. The glass disks were arranged in a square array with a clear spacing between them equal to one-half the disk radius. They were cemented to one side of the mold by means of Duco cement to prevent them from sliding. The mold was closed with a glass plate and the resin poured from the top. Care was taken to prevent air bubbles from forming and adhering to the inclusions. The resin was allowed to cure in the mold at room temperature. Four two-dimensional specimens, 30.5 cm (12.0 in.) long, 8.25 cm (3.25 in.) wide and 0.60 cm (0.24 in.) thick, were prepared.

The same matrix was used in preparing unidirectional prototype composite specimens with glass fibers (G filament size.) Six layers of glass roving were wound around an open metal frame of dimensions 35.6 cm x 44.5 cm (14 in. x 17.5 in.) in a filament winding machine. Resin was brushed on each layer of glass fibers during winding. A total of 180g of resin was used for the six layers. Seventy-five minutes after first mixing the resin and the hardener, the wet layup was placed over a 0.051 mm (0.002 in.) thick teflon film and was covered with a layer of TX 1040 separator (teflon coated glass scrim cloth), two layers of style 1581 glass bleeder cloth, a 0.051 mm (0.002 in.) thick teflon film with perforations, and a layer of style 1581 glass vent cloth. The assembly was placed between two steel pressure plates in a

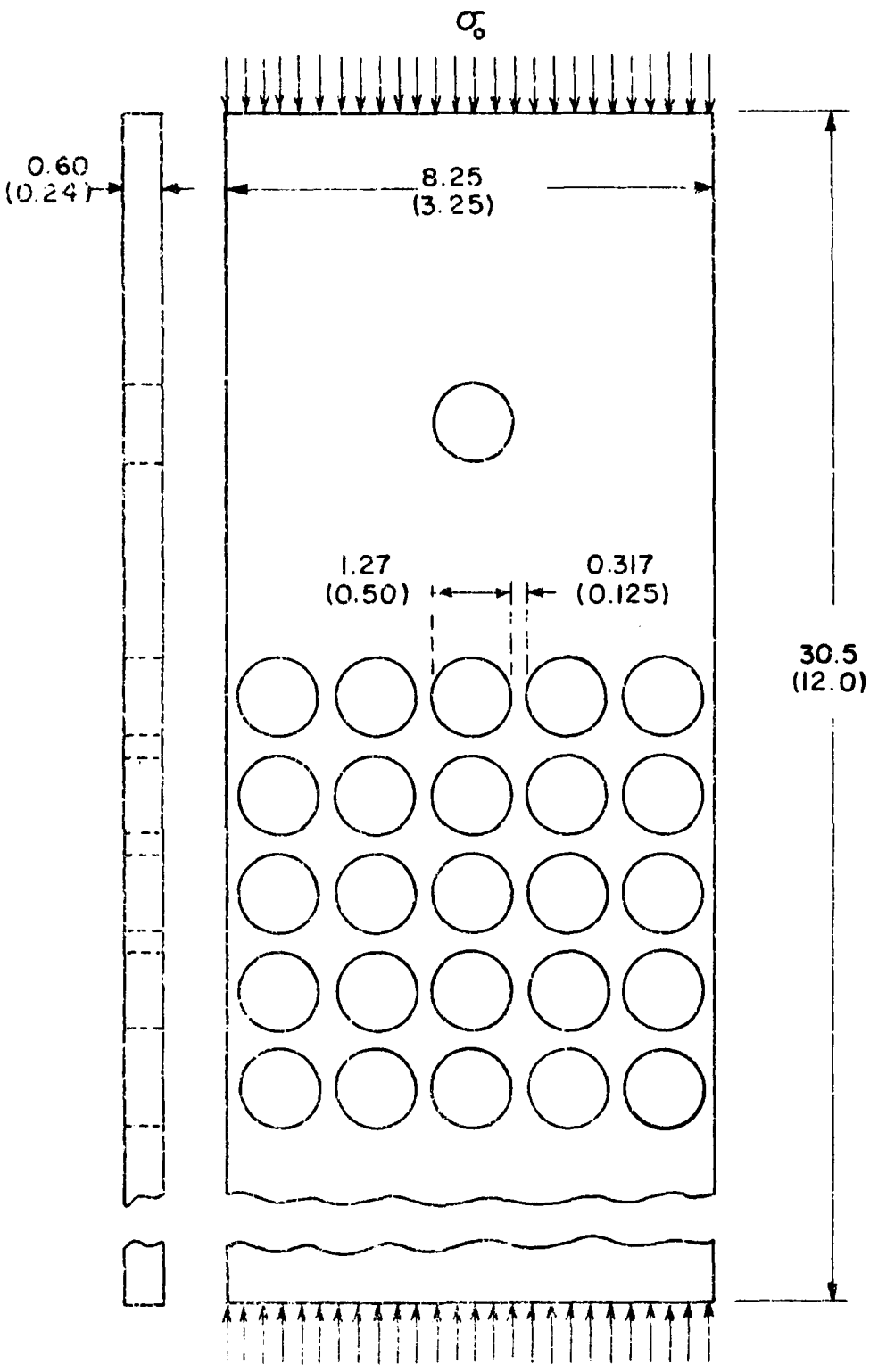

Figure 1

Two-Dimensional Photoelastic Model for Determination of Internal Stress Distributions in Composites
(Dimensions are in centimeters and inches)

blanket press. Full vacuum was drawn and a 207 kPa (30 psi) pressure applied. After thirty minutes the vacuum pump was shut off and the plate was vented to atmosphere. The plate was then allowed to cure at room temperature overnight. Three 27.9 cm x 33.0 cm x 0.173 cm (11 in. x 13 in. x 0.068 in.) unidirectional plates were fabricated. Coupons, 2.54 cm (1 in.) wide and 22.9 cm (9 in.) long, were machined from these plates with their longitudinal axis perpendicular to the fiber direction.

3. MATRIX MATERIAL CHARACTERIZATION

Mechanical and optical properties were determined at room temperature for the matrix material used in the preparation of the specimens. The material was characterized after curing at room temperature and after post-curing at 339 degK (150°F) and 367 degK (200°F).

Mechanical properties were determined by testing under uniaxial tension dogbone specimens instrumented with strain gages. These specimens had a gage section 10.2 cm (4 in.) long, 0.76 cm (0.30 in.) wide and 0.53 cm (0.21 in.) thick. Stress-strain curves for a room-temperature cured specimen two weeks and four weeks after casting and a postcured specimen are shown in Figs. 2, 3, and 4. No significant differences were found in the elastic properties among the three specimens. The average modulus and Poisson's ratio for the matrix material are:

E = 3 84 GPa (0.557×10^6 psi)
ν = 0.36

The measured tensile strengths were:

S_T = 45.3 MPa (6,560 psi) (room temperature cured)
S_T = 83.1 MPa (12,050 psi) (post-cured at 339 degK, 150°F)
S_T = 86.9 MPa (12,600 psi) (post-cured at 367 degK, 200°F)

The material fringe value was determined by testing disks under diametral compression and using the following relation:

$$f = \frac{4P}{\pi D n} \qquad (1)$$

where

f = material fringe value, kPa-m/fringe $\left(\frac{\text{psi -in.}}{\text{fringe}}\right)$
P = diametral load, N (lb)
D = disk diameter

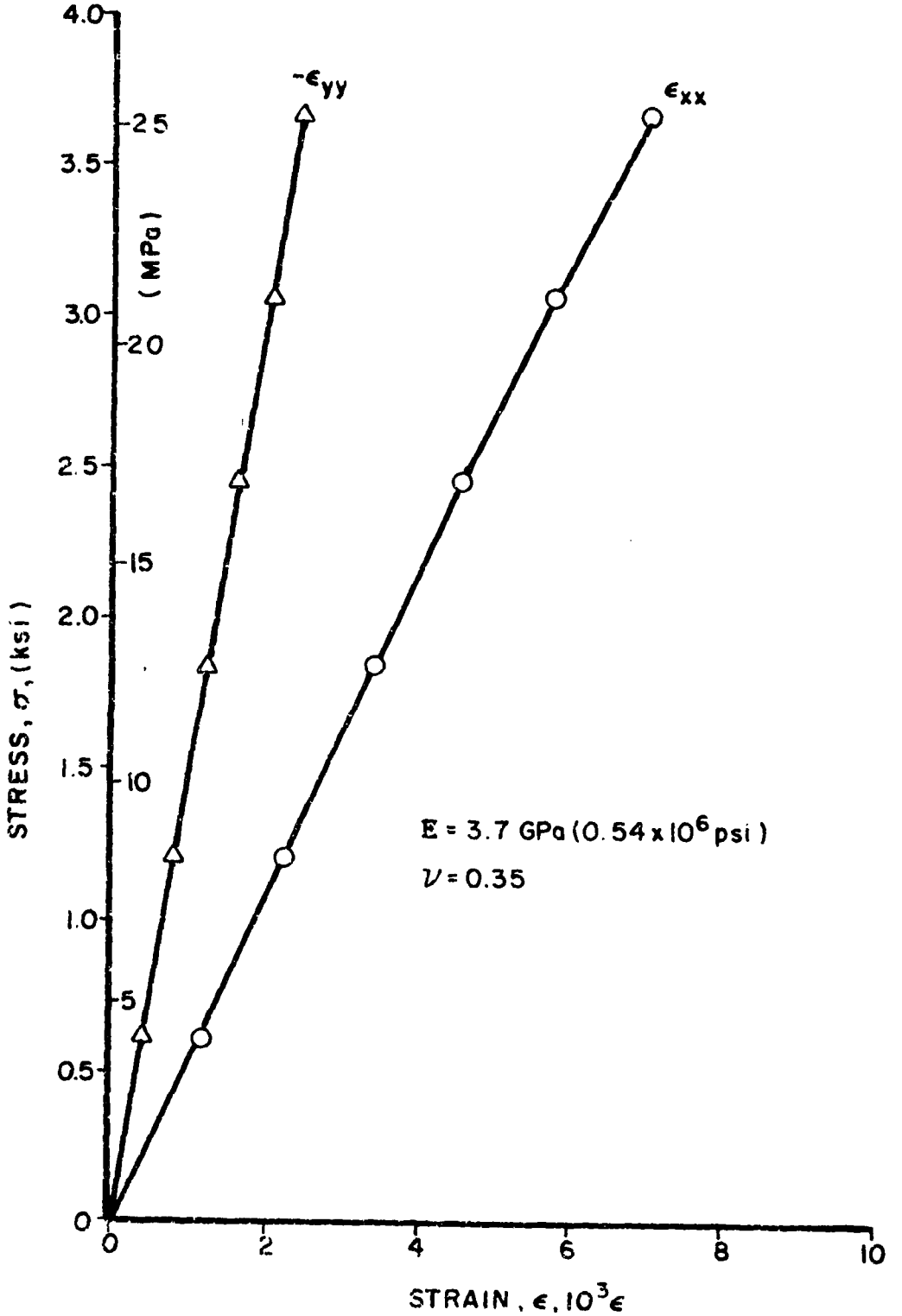

Figure 2
Stress-Strain Curves for DER 332 Epoxy Resin.
Specimen No. 2-18-DB1 (Room-Temperature Cured,
Tested Two Weeks after Casting)

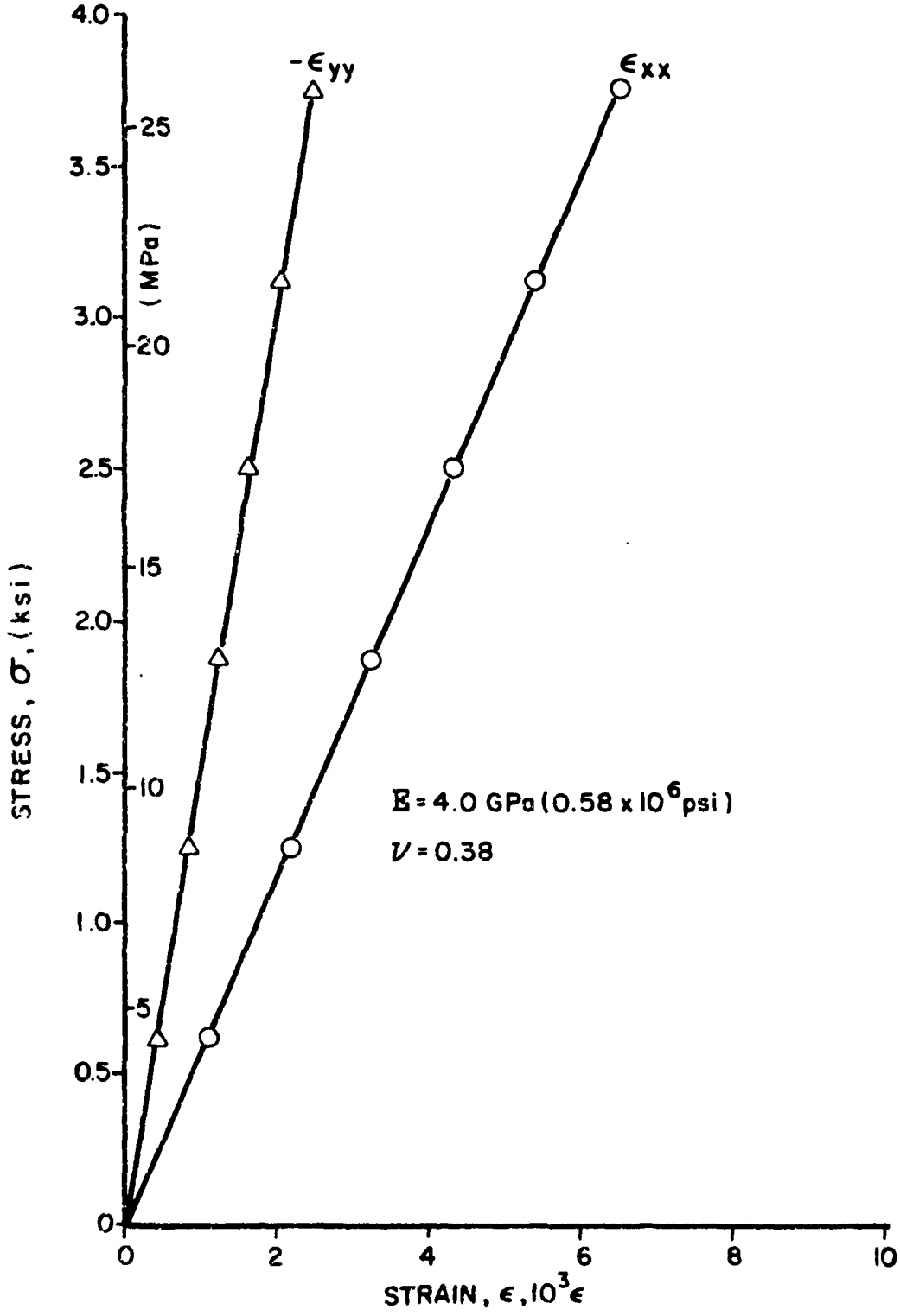

Figure 3

Stress-Strain Curves for DER 332 Epoxy Resin. Specimen No. 1-18-DB1 (Room-Temperature Cured, Tested Four Weeks after Casting)

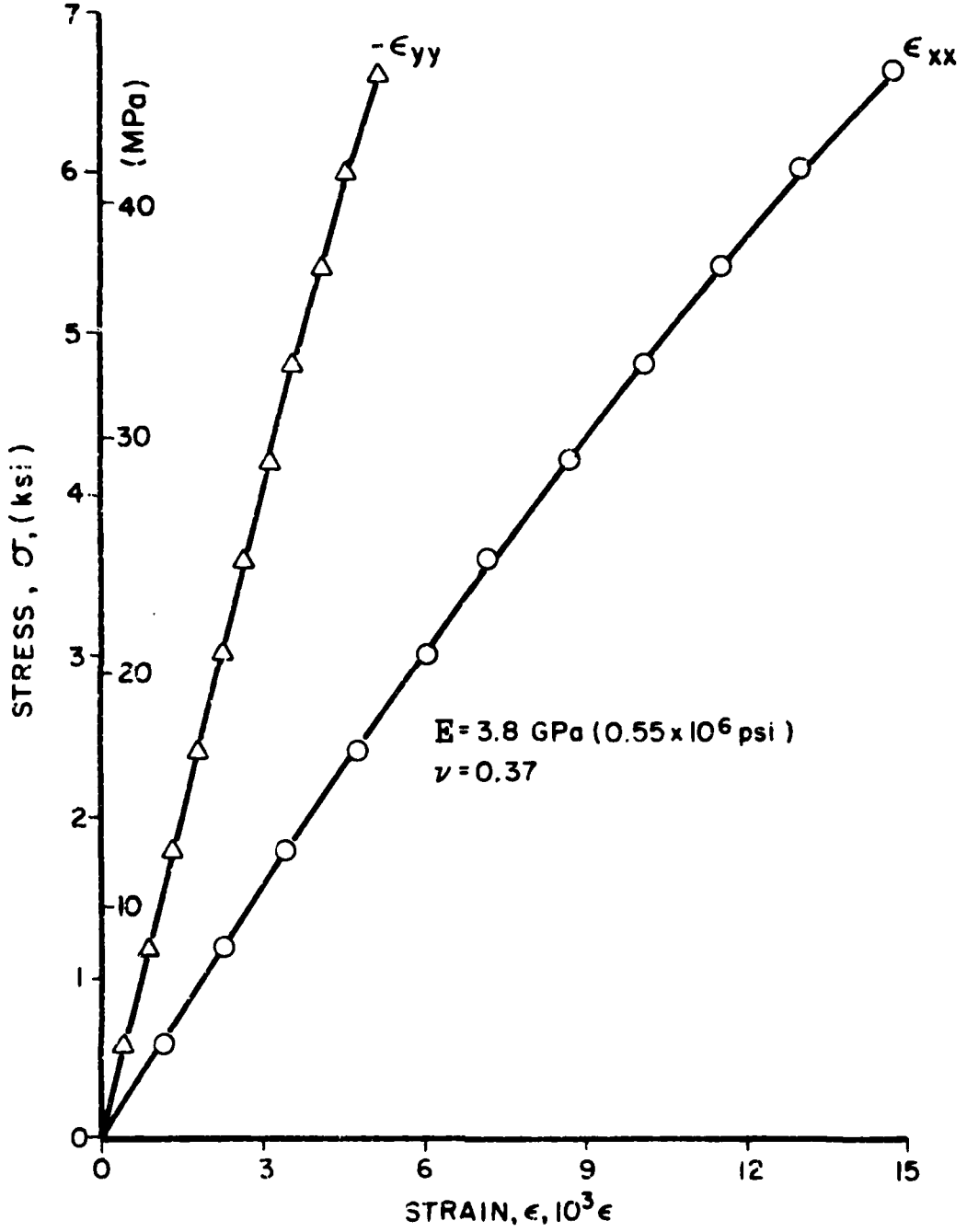

Figure 4

Stress-Strain Curves for DER 332 Epoxy Resin. Specimen No. 1-17 DB1 (Post-Cured at 367 degK, 200°F)

n = fringe order at center of disk

A typical load-birefringence curve for a room temperature-cured disk is shown in Fig. 5. Fringe values obtained from such calibration tests are:

f = 8.75 kPa-m/fringe (50.0 psi-in/fringe) (room temperature cured)
f = 8.05 kPa-m/fringe (46.0 psi-in/fringe) (post-cured, 339°K)
f = 6.90 kPa-m/fringe (39.4 psi-in/fringe) (post-cured, 367°K)

The variation of fringe value with post-cure temperature is shown in Fig. 6.

The density of the matrix resin determined by weighing a disk of the material and measuring its volume is:

$\rho_m = 1,190 \text{ kg/m}^3$

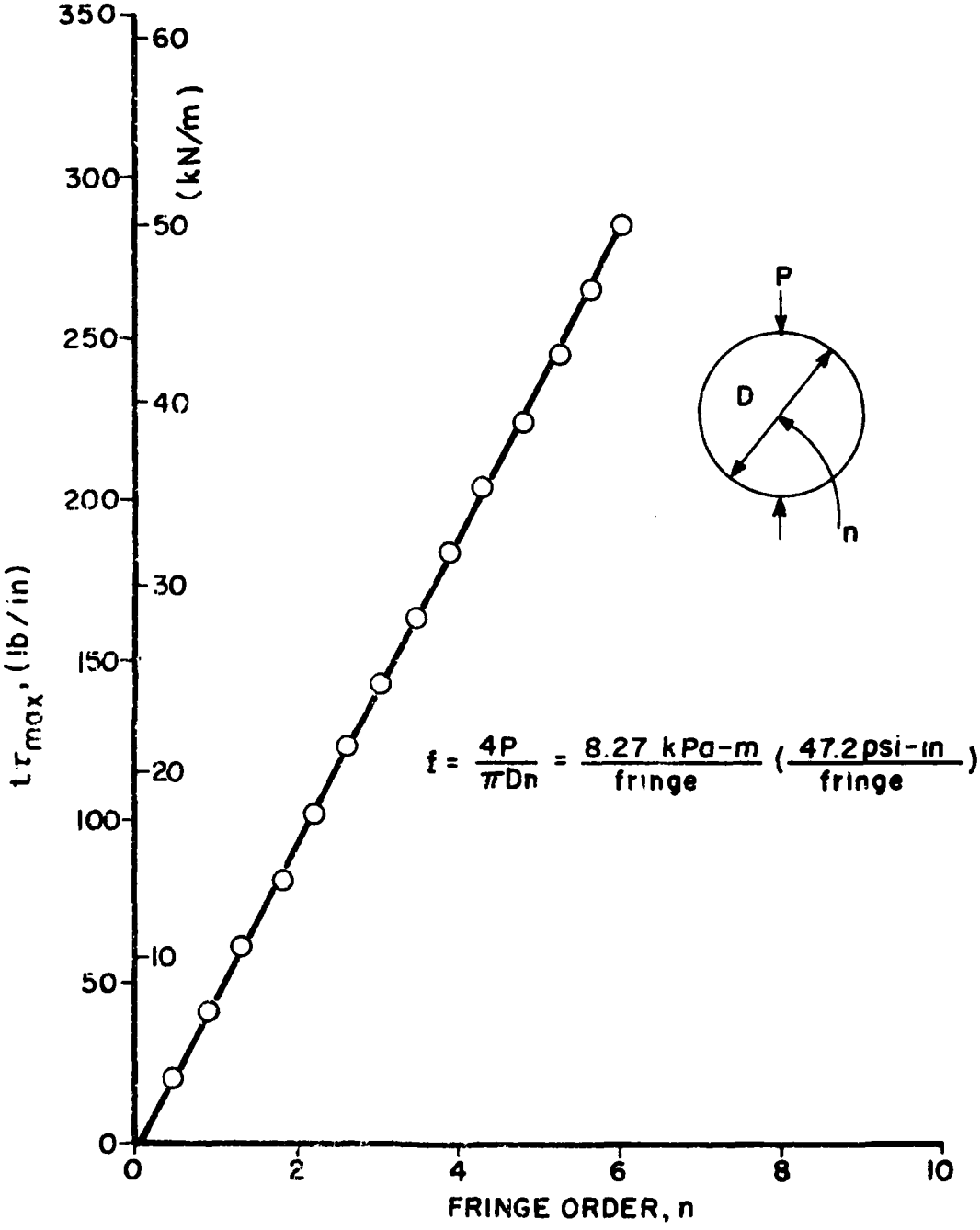

Figure 5

Load-Fringe Order Curve for DER 332 Epoxy Resin. Specimen No. 1-18-D1 (Room-Temperature Cured, Tested Two Weeks after Casting)

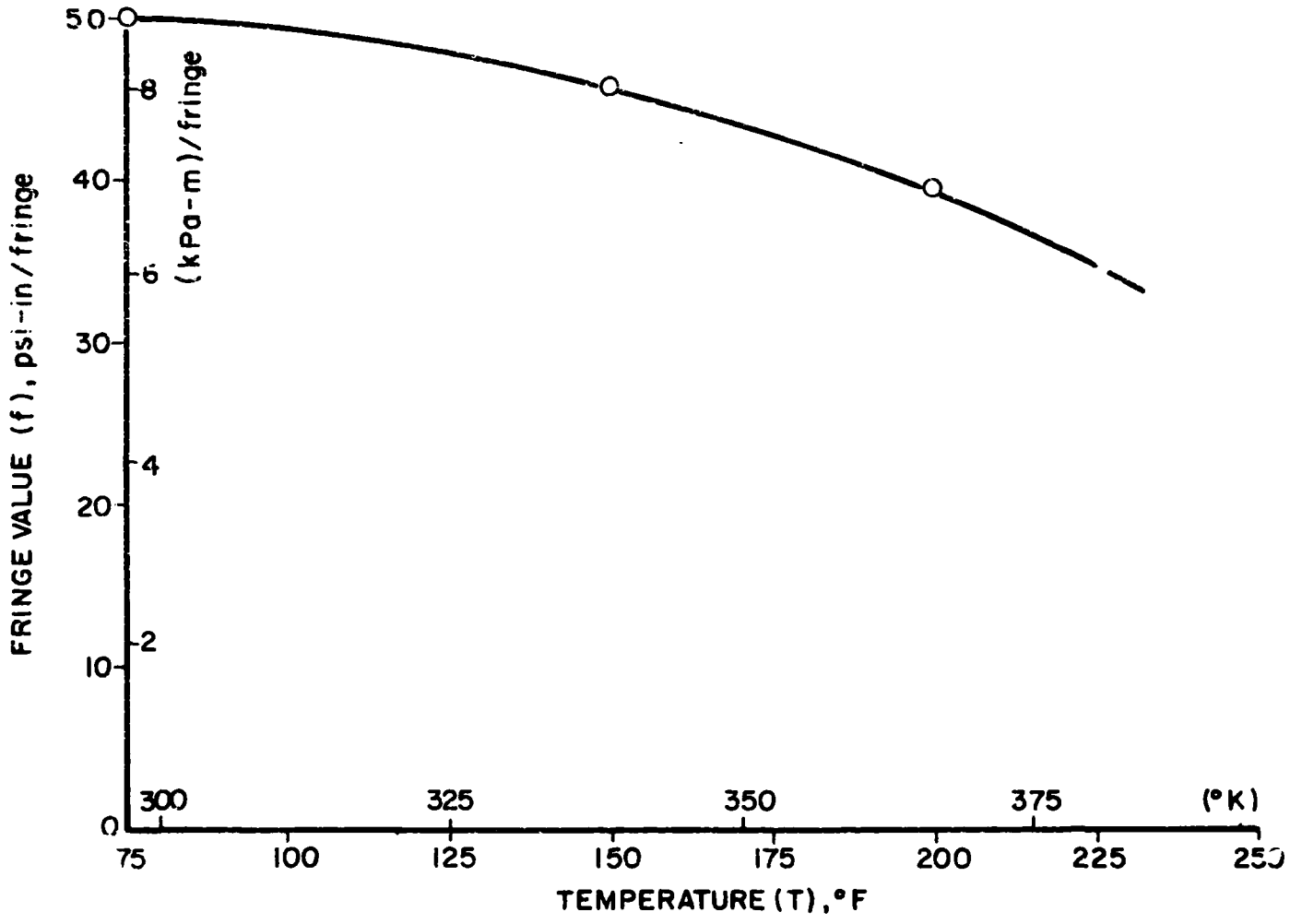

Figure 6

Fringe Value for DER 332 Epoxy Resin as a Function of Post-cure Temperature

4. EVALUATION OF RESIDUAL STRESSES

The state of residual stress in the model and prototype composite specimens can be determined photoelastically and described in dimensionless form by dividing the actual stresses by the nominal interface pressure around a single isolated inclusion. Experimental and analytical solutions exist for this dimensionless stress distribution for a composite of 0.50 fiber volume ratio.[29] Stress distributions obtained from a three-dimensional photoelastic model along two axes of symmetry are shown in Figs. 7 and 8.

To determine the exact magnitude of residual stresses in any other composite model with a 0.50 equivalent fiber volume ratio it is necessary to multiply the dimensionless stresses above by the residual stress σ_o^R at the interface of an isolated inclusion.

Thus, the principal residual stress components at the interface along an axis of symmetry through the fibers are (Fig. 8):

$$\begin{aligned} \sigma_\theta &= 0.8\ \sigma_o^R \\ \sigma_r &= -2.0\ \sigma_o^R \\ \sigma_z &= 0.9\ \sigma_o^R \end{aligned} \tag{2}$$

The interface stress around a single isolated fiber is obtained from the fringe order around a single inclusion as follows:

$$\sigma_o^R = \frac{n_o^R f}{t} \tag{3}$$

where n_o^R is the maximum fringe order at the interface of a single inclusion, f the material fringe value and t the specimen thickness.

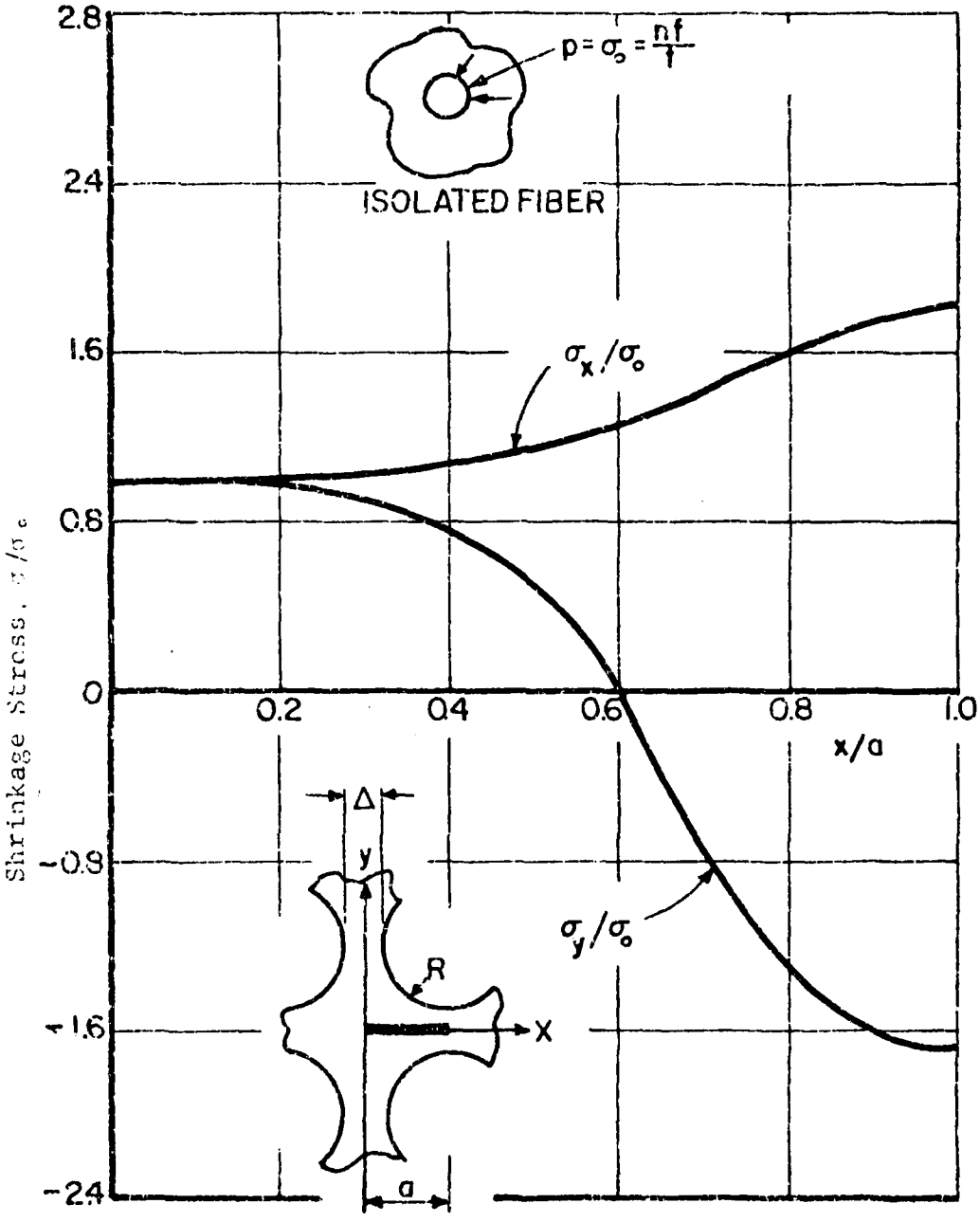

Figure 7

Distribution of Shrinkage Stress
Along Ligament Centerline, Δ/R = .50

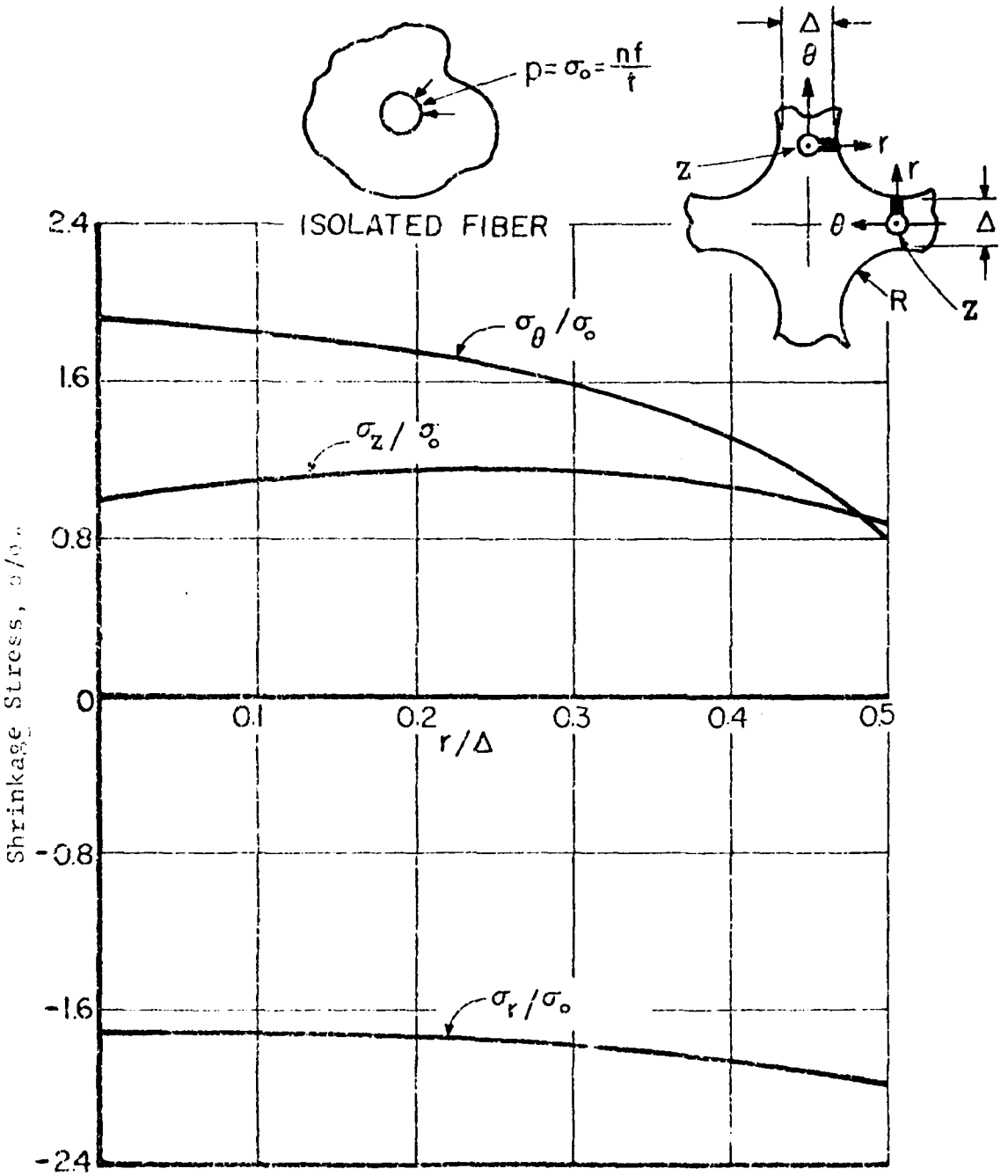

Figure 8

Distribution of Shrinkage Stresses Across Section Between Fibers, Δ/R = .50

Typical values for the photoelastic models used in this study for a room temperature-cured matrix are:

$$n_o^R = 1.35$$
$$f = 8.75 \text{ kPa-m/fringe } (50.0 \text{ psi-in/fringe})$$
$$t = 0.592 \text{ cm } (0.233 \text{ in.})$$

Substituting in Eqs. (3) and (2) we obtain:

$$\sigma_\theta = 1{,}600 \text{ kPa } (230 \text{ psi})$$
$$\sigma_r = -4{,}000 \text{ kPa } (-580 \text{ psi})$$
$$\sigma_z = 1{,}800 \text{ kPa } (260 \text{ psi})$$

The octahedral shear stress, commonly used as a failure criterion, is

$$\tau_{oct}^R = \frac{\sigma_o^R}{3}\left[(2.8)^2 + (2.9)^2 + (0.1)^2\right]^{1/2} = 1.344\sigma_o^R \qquad (4)$$

The residual strain components at the matrix-fiber interface along the axis of symmetry through the fibers are:

$$\varepsilon_\theta = \frac{\sigma_o^R}{E}(0.8 + 1.1\nu)$$
$$\varepsilon_r = \frac{\sigma_o^R}{E}(2.0 + 1.7\nu) \qquad (5)$$
$$\varepsilon_z = \frac{\sigma_o^R}{E}(0.9 + 1.2\nu)$$

The corresponding octahedral shear strain is:

$$\gamma_{oct}^R = \frac{2(1+\nu)}{E}\tau_{oct}^R \qquad (6)$$

The state of residual stress depends on the curing cycle. For the resin used here, a simple way to produce different magnitudes of residual stress is to post-cure the room temperature-cured resin at different elevated temperatures. The easiest way

to determine the magnitude of residual stress as discussed before is to measure the birefringence around a single isolated inclusion. Figure 9 shows residual birefringence around isolated glass disk inclusions in a resin cured at room temperature and post-cured at various elevated temperatures. The variation of maximum fringe order and residual stress at the interface with post-cure temperature is illustrated in Fig. 10. The variation of fringe value with post-cure temperature was taken into account in calculating the interface residual stress.

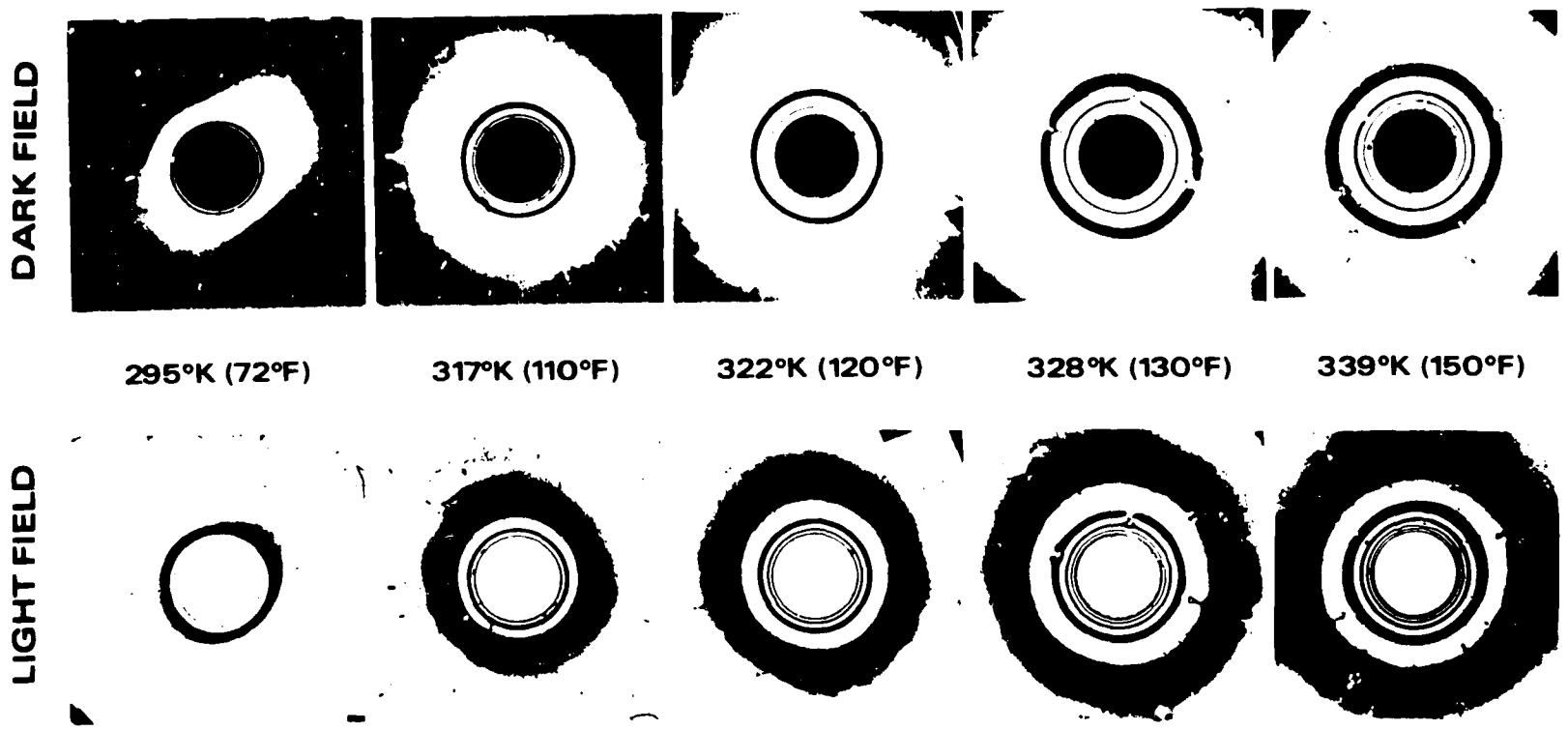

Figure 9

Fringe Patterns Around Single Isolated Inclusions
in Resin Post-cured at Different Temperatures

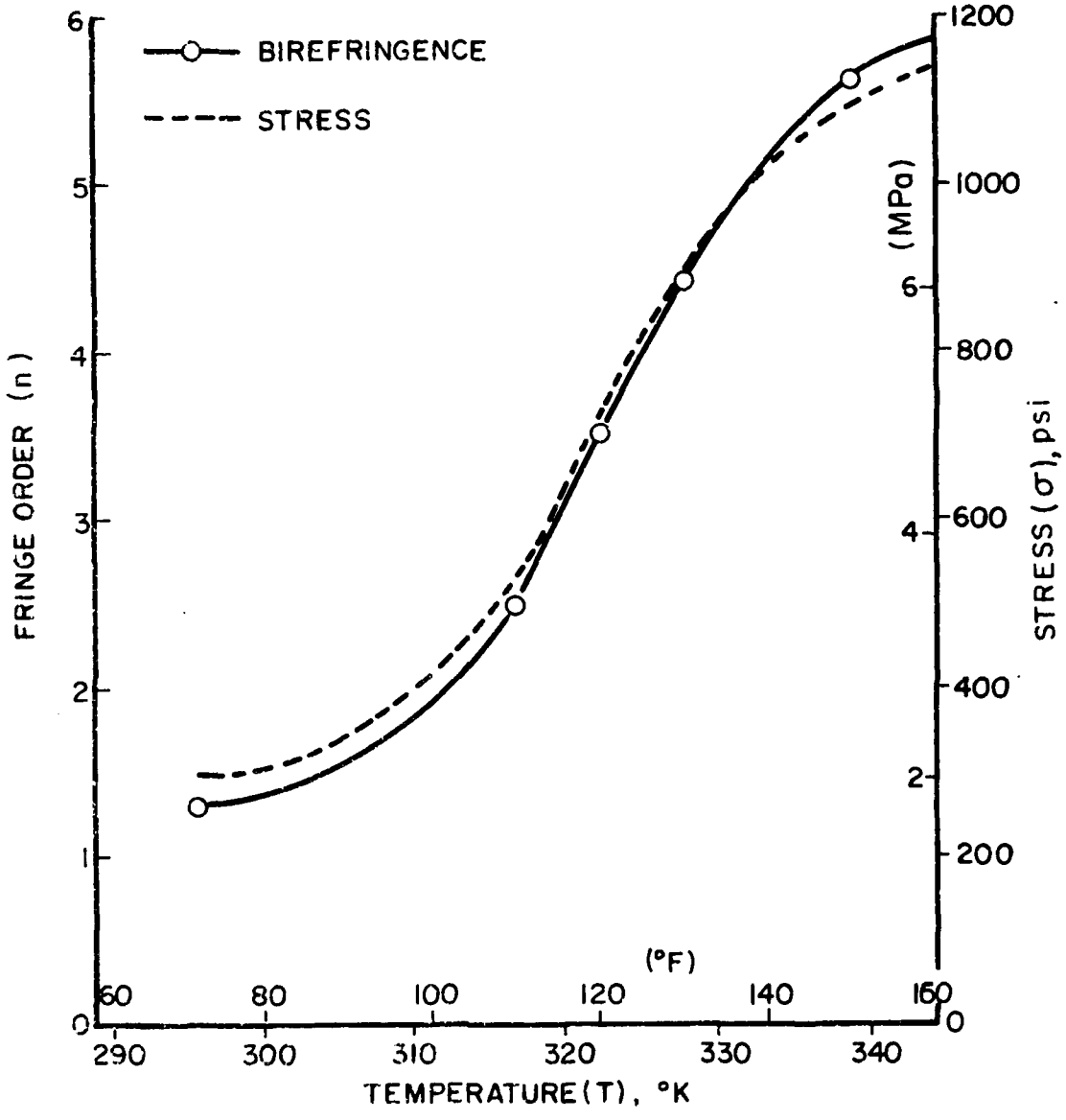

Figure 10

Maximum Fringe Order and Interface Pressure Around a Single Isolated Inclusion as a Function of Post-cure Temperature.

5. INTERNAL STRESS DISTRIBUTION UNDER EXTERNAL LOADING

The two-dimensional photoelastic models of the transverse cross-section of a unidirectional composite (Fig. 1) were loaded in uniaxial compression in the plane of the model. A loading fixture was used to apply uniform pressure along the two opposite edges of the model (Fig. 11). A compression loading was selected to avoid the possibility of cracking or debonding of the resin around the inclusions which might occur under tensile loading. It is easier to control the uniformity of compressive loading when applied by means of hydraulic pressure. From the point of view of stress analysis, within the elastic range, the stress distribution is the same for tension or compression except for the sign of the stresses.

The loading fixture is essentially a four-member frame consisting of two vertical supports and two horizontal pressure sections. The pressure section is a sandwich of three steel plates securely fastened to each other by means of bolts. The thickness of the central plate is approximately equal to the thickness of the model. This central plate is recessed from the outer plates to accommodate a flexible rubber tube and the loaded edge of the specimen. To prevent buckling of the specimen under the applied compressive loads, two pairs of anti-buckling bars were placed horizontally across the plate and fastened to the vertical members of the frame. A small clearance of approximately 0.127 mm (0.005 in.) was provided between these bars and the specimen.

The specimens were inserted in place by lowering the lower pressure section by means of the large bolts at the base. A source of high pressure nitrogen gas was used to pressurize the rubber tubing. Although the pressure in the rubber tubing was measured accurately with a pressure gage, it is known that the effective pressure loading on the specimen is slightly lower than the measured pressure. The ineffective pressure is determined by

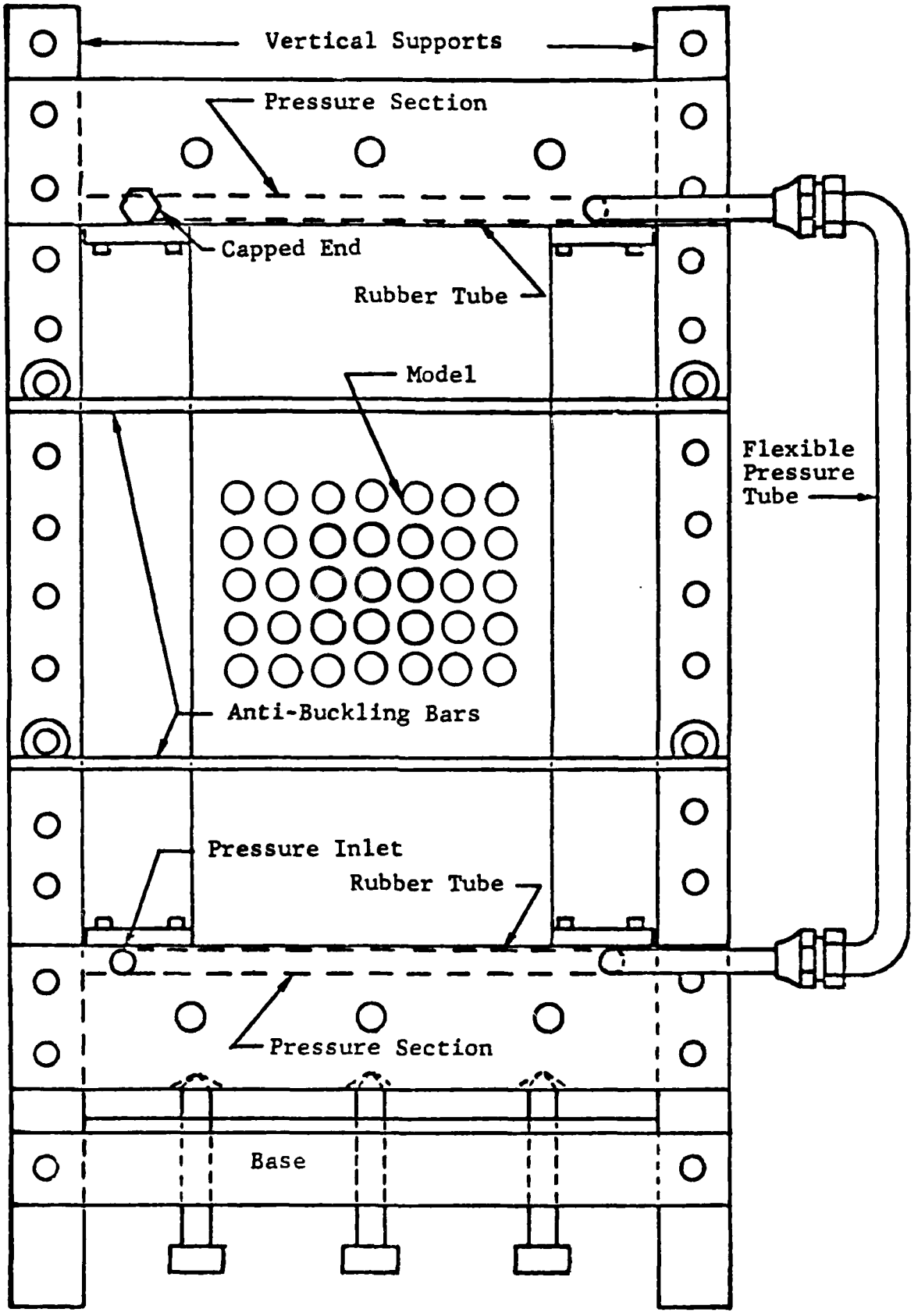

Figure 11

Fixture for Uniaxial Loading
of Photoelastic Specimens

plotting the apparent pressure versus a fringe order and measuring the vertical intercept on the pressure axis at the zero (load-induced) fringe order.

Two specimens were subjected to five levels of load. Dark field and light field isochromatic fringe patterns around the inclusions were photographed and birefringence readings were taken at 0 kPa (0 psi), 1,380 kPa (200 psi), 2,760 kPa (400 psi), 4,140 kPa (600 psi), 5,520 kPa (800 psi), and 6,900 kPa (1,000 psi) gage pressures (Figs. 12 and 13). The two specimens differ in the amount of initial birefringence or residual stress.

The data of interest in testing these models were the maximum fringe order n_1 at the boundary of one of the central inclusions of the array along the vertical diameter and the fringe order n_o at a similarly located point around the single isolated inclusion. The variation of these two fringe orders with applied stress is shown in Figs. 14 and 15 for the two specimens tested. The ineffective part of the applied pressure has been subtracted in these graphs. The horizontal intercepts on the fringe order axis represent initial birefringence due to residual stress.

The state of stress in the matrix of the two-dimensional specimens is a complex three-dimensional one due to the out-of-plane restraint introduced by the inclusions at their interface. Away from the interface, the state of stress tends to approach the plane stress condition. In two-dimensional photoelastic analyses, the birefringence measured is related to the in-plane stresses averaged over the thickness (optical path) of the specimen. Stress-strain relations can be expressed in terms of these values by integrating them through the thickness of the specimen.

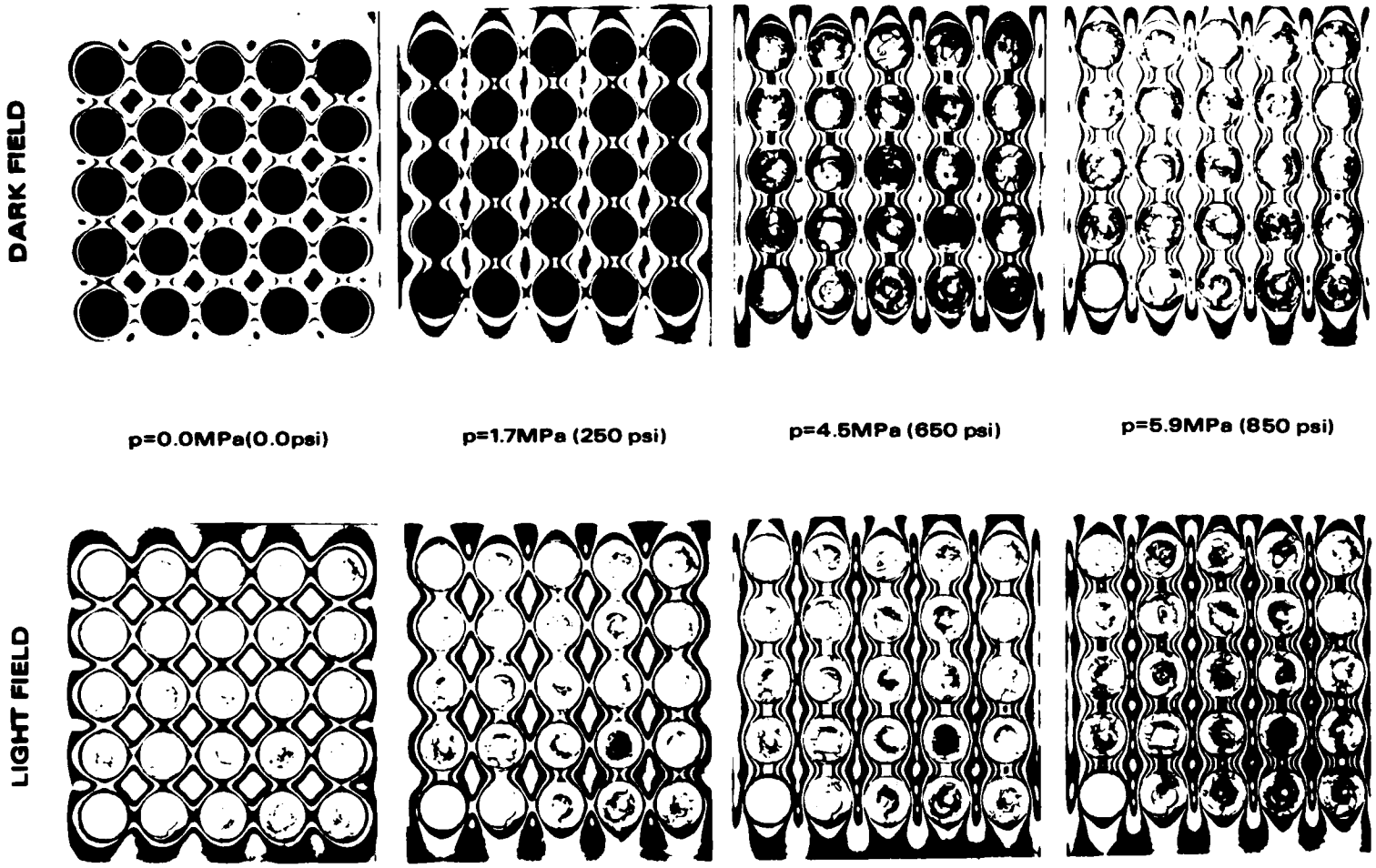

Figure 12
Isochromatic Fringe Patterns for Composite Model
with Square Array of Inclusions Under Uniaxial Loading
(Specimen No. 10)

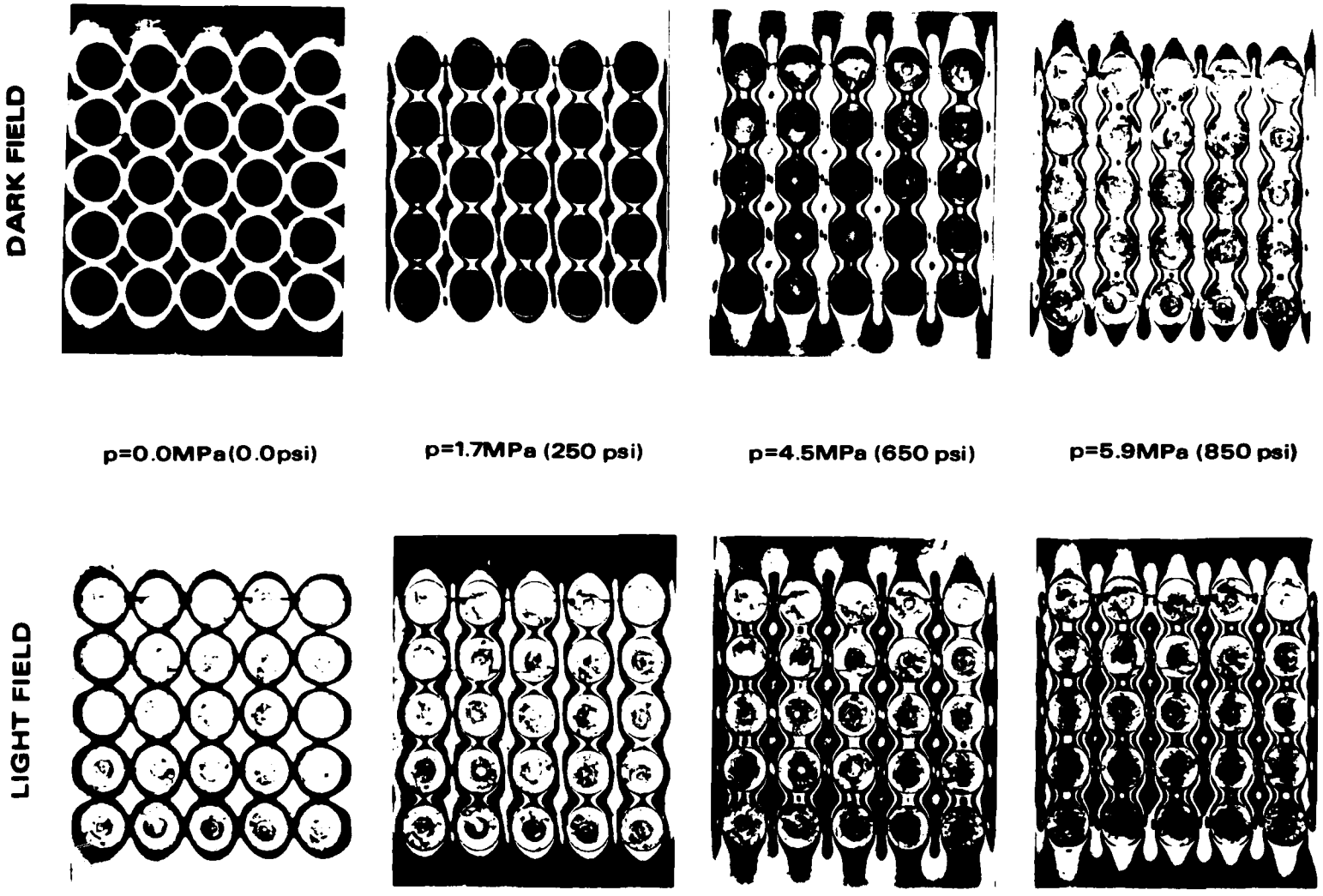

Figure 13
Isochromatic Fringe Patterns for Composite Model
with Square Array of Inclusions Under Uniaxial Loading
(Specimen No. 11)

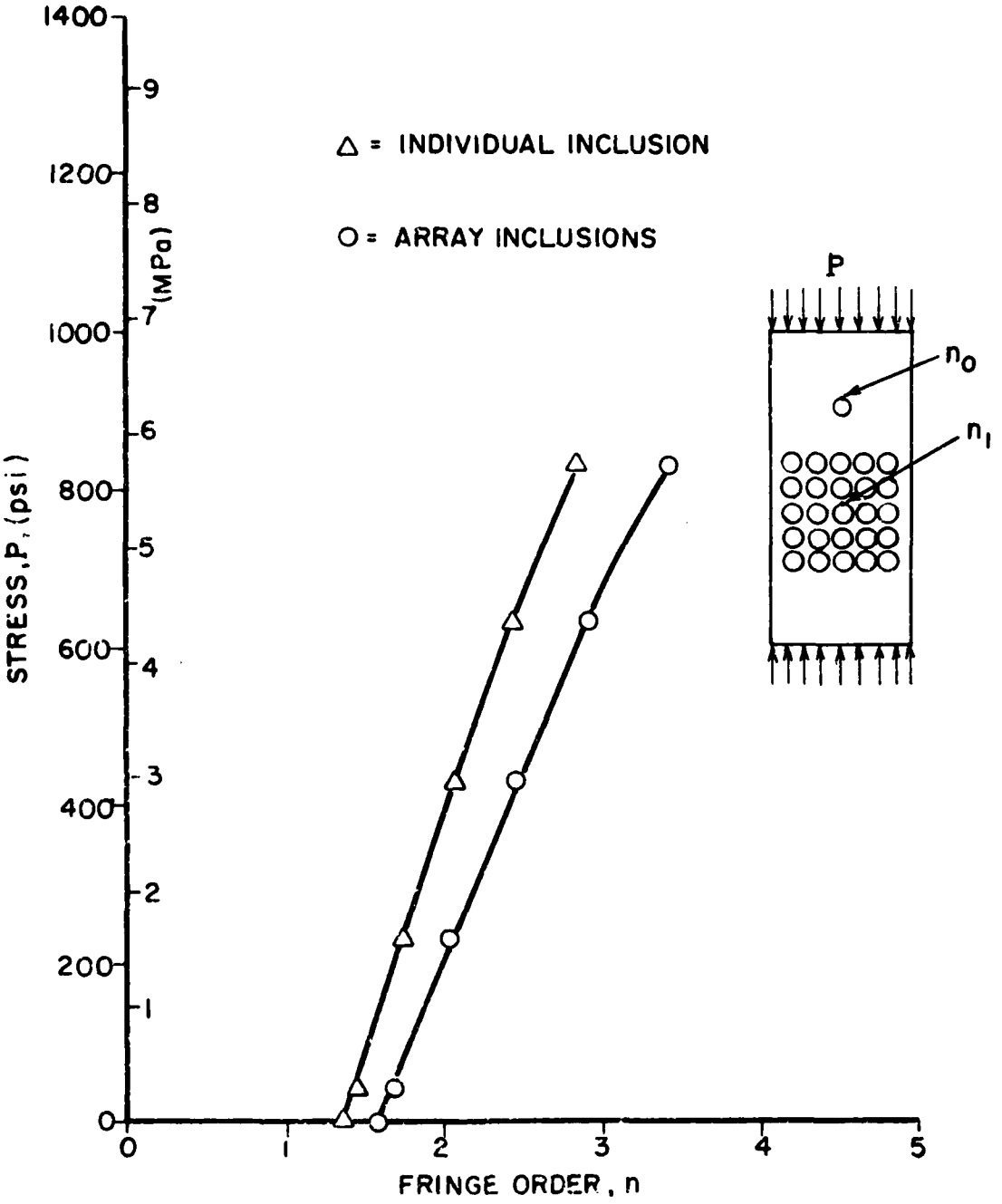

Figure 14

Stress-Birefringence Curves for Photoelastic Specimen with 1.27 cm (0.50 in.) Inclusion Array (Specimen No. 10)

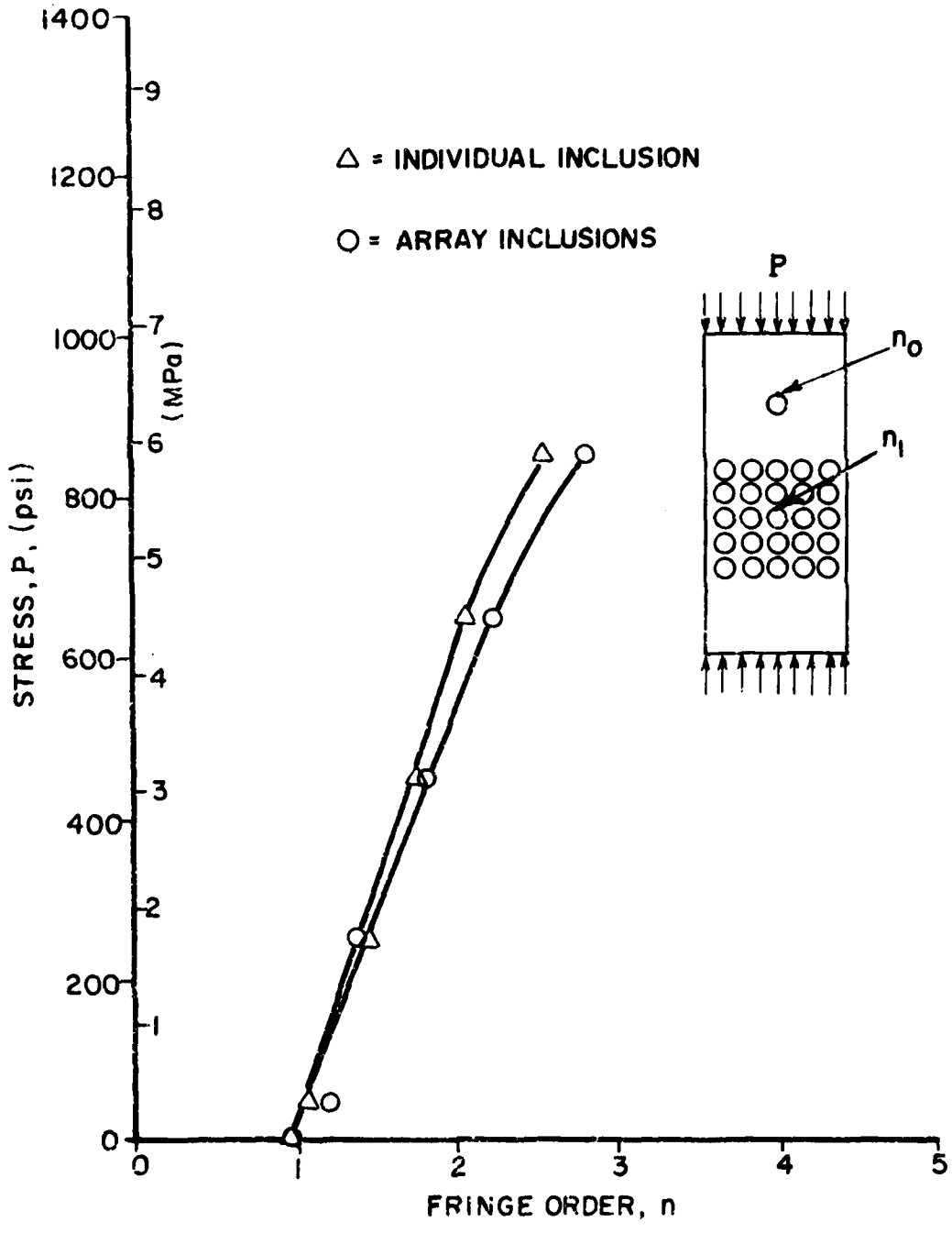

Fringe 15

Stress-Birefringence Curves for Photoelastic Specimen with 1.27 cm (0.50 in.) Inclusion Array (Specimen No. 11)

$$\left.\begin{aligned}
\bar{\sigma}_x &= \frac{E}{(1+\nu)(1-2\nu)}\left[(1-\nu)\,\bar{\varepsilon}_x + \nu(\bar{\varepsilon}_y + \bar{\varepsilon}_z)\right] \\
\bar{\sigma}_y &= \frac{E}{(1+\nu)(1-2\nu)}\left[(1-\nu)\,\bar{\varepsilon}_y + \nu(\bar{\varepsilon}_x + \bar{\varepsilon}_z)\right] \\
\bar{\sigma}_z &= \frac{E}{(1+\nu)(1-2\nu)}\left[(1-\nu)\,\bar{\varepsilon}_z + \nu(\bar{\varepsilon}_x + \bar{\varepsilon}_y)\right]
\end{aligned}\right\} \tag{7}$$

where $\bar{\sigma}_x$, $\bar{\sigma}_y$, $\bar{\varepsilon}_x$, $\bar{\varepsilon}_y$, are in-plane stresses and strains transverse and parallel to loading direction and averaged through the thickness of the specimen; $\bar{\sigma}_z$ and $\bar{\varepsilon}_z$ are the out-of-plane stress and strain averaged through the thickness.

The inclusions can be considered rigid compared with the matrix due to the high ratio of moduli. This fact introduces the following condition on the boundary of the inclusion on the vertical axis of symmetry where the maximum stress occurs:

$$\bar{\varepsilon}_x = \bar{\varepsilon}_z = 0 \tag{8}$$

From Eqs. (7), it follows that

$$\bar{\sigma}_x = \bar{\sigma}_z = \frac{\nu}{1-\nu}\,\bar{\sigma}_y \tag{9}$$

Substituting in the stress-optic law of photoelasticity

$$\bar{\sigma}_x - \bar{\sigma}_y = \frac{2n_1 f}{t} \tag{10}$$

we obtain

$$\bar{\sigma}_y = \left(\frac{1-\nu}{1-2\nu}\right)\frac{2n_1 f}{t} \tag{11}$$

and

$$\bar{\sigma}_x = \bar{\sigma}_z = \frac{\nu}{1-2\nu}\,\frac{2n_1 f}{t} \tag{12}$$

The maximum stress at the interface was calculated from the measured fringe order using Eq. (11). The stress concentration

factor obtained by dividing the interface stress by the applied average stress is:

$$k_\sigma = \frac{\bar{\sigma}_y}{\sigma_o} = 1.95 \tag{13}$$

which is very close to similar values obtained by Adams[30] and Marloff and Daniel.[29] The stress concentration value above is very sensitive to the value of Poisson's ratio for the material because of the $(1 - 2\nu)$ factor in the denominator of Eq. (11). For a Poisson's ratio of $\nu = 0.37$ the stress concentration factor becomes 2.04.

The quantity of importance in transversely loaded composites is the strain concentration factor in the matrix since many failures originate in the matrix. This factor is defined as the ratio of the maximum interface radial strain to the average strain in the composite model.

$$k_\varepsilon = \frac{\bar{\varepsilon}_y}{\varepsilon_o} \tag{14}$$

From the relation

$$\bar{\varepsilon}_x - \bar{\varepsilon}_y = \frac{1 + \nu}{E} (\bar{\sigma}_x - \bar{\sigma}_y) \tag{15}$$

the boundary condition,

$$\bar{\varepsilon}_x = 0$$

and Eqs. (11) and (12) it follows that

$$\bar{\varepsilon}_y = \frac{(1 + \nu)(1 - 2\nu)}{E(1 - \nu)} \bar{\sigma}_y \tag{16}$$

The nominal strain is

$$\varepsilon_o = \frac{\sigma_o}{E_c} \tag{17}$$

where σ_o = average stress

E_c = transverse composite modulus

Then, the strain concentration factor is expressed as

$$k_\varepsilon = \frac{\bar{\varepsilon}_y}{\varepsilon_o} = k_\sigma \frac{E_c}{E} \frac{(1 + \nu)(1 - 2\nu)}{(1 - \nu)} \tag{18}$$

For $\nu = 0.36$, $k_\varepsilon = 0.595\, k_\sigma \left(\frac{E_c}{E}\right)$

Of the quantities entering expression (18), k_σ is obtained from photoelastic data only, E and ν are obtained from characterization tests of the matrix material and E_c is either calculated or measured directly in the model or in a prototype material of the same fiber volume ratio.

6. PREDICTION OF TRANSVERSE TENSILE STRENGTH

6.1 Maximum Tensile Strain Criterion

The maximum strain at the interface of a fiber due to combined transverse tensile loading and curing is obtained by adding the strains from Eqns. (5) and (16);

$$(\varepsilon_y)_{max} = (\varepsilon_r)_{max} = \frac{(1 + \nu)(1 - 2\nu)}{E(1 - \nu)} k_\sigma \sigma_o - \frac{\sigma_o^R}{E}(2 + 1.7\nu) \quad (19)$$

Equating this strain to the ultimate tensile strain in the resin and assuming linear elastic behavior to failure, we obtain:

$$\varepsilon^u = \frac{S_T}{E} = (\varepsilon_y)_{max} \quad (20)$$

Solving for σ_o in the equations above and equating it to the transverse tensile strength of the unidirectional composite we obtain:

$$\sigma_o = S_{22T} = \frac{(1 - \nu)}{k_\sigma (1 + \nu)(1 - 2\nu)} \left[S_T + \sigma_o^R (2 + 1.7\nu) \right] \quad (21)$$

Substituting the values S_T = 45.3 MPa (6,560 psi), σ_o^R = 2 Mpa (290 psi) and ν = 0.36, we obtain:

S_{22T} = 43.5 MPa (6310 psi).

This value is very sensitive to the value of Poisson's ratio used, because of the (1 - 2ν) factor in the denominator of Eq. (21). For ν = 0.37 the predicted strength becomes S_{22T} = 46.9 MPa (6,790 psi).

For a matrix material postcured at 339°K (150°F), S_T = 83.1 Mpa (12,050 psi) and σ_o^R = 7.6 MPa (1096 psi). Then

S_{22T} = 88.7 MPa (12,850 psi).

6.2 Octahedral Shear Stress Criterion

The three principal stress components at the fiber matrix interface due to combined transverse tensile loading and curing shrinkage are obtained from Eqns. (2) and (4):

$$\sigma_x = \frac{\nu}{1-\nu} k_\sigma \sigma_o + 0.8 \sigma_o^R$$

$$\sigma_y = k_\sigma \sigma_o - 2\sigma_o^R \qquad (22)$$

$$\sigma_z = \frac{\nu}{1-\nu} k_\sigma \sigma_o + 0.9\sigma_o^R$$

The octahedral shear stress then is given by:

$$\tau_{oct} = \frac{1}{3}\sqrt{(\sigma_x - \sigma_y)^2 + (\sigma_y - \sigma_z)^2 + (\sigma_z - \sigma_x)^2} \qquad (23)$$

The octahedral shear stress for the uniaxially loaded matrix material is given by

$$\tau_{oct} = \frac{\sqrt{2}}{3} S_T \qquad (24)$$

Equating Eqns. (23) and (24) and using Eqns. (22) we obtain:

$$\left(\frac{1-2\nu}{1-\nu}\right)^2 k_\sigma^2 \sigma_o^2 - 5.7\left(\frac{1-2\nu}{1-\nu}\right) k_\sigma \sigma_o^R \sigma_o + 8.13 \left(\sigma_o^R\right)^2 - S_T^2 = 0 \qquad (25)$$

Substituting the values S_T = 45.3 MPa (6,560 psi), σ_o^R = 2 MPa (290 psi) and ν = 0.36 and solving for σ_o we obtain:

$$\sigma_o = S_{22T} = 59.7 \text{ MPa } (8\,660 \text{ psi}).$$

The corresponding value of the predicted strength for the postcured resin is

S_{22T} = 122.7 MPa (17,780 psi).

6.3 Prototype Composite Tests

Unidirectional [90_6] coupons of glass/epoxy having the same matrix as the photoelastic models, the same fiber volume ratio, and cured at room temperature were tested in tension to failure. The coupons were 2.54 cm (1 in.) wide and 22.9 cm (9 in.) long. They were insturmented with a two-gage rosette on each side. Stress-strain curves to failure for two such coupons are shown in Figs. 16 and 17. Average results obtained from seven such test

E_{22} = 12.6 GPa (1.83×10^6 psi)

ν_{21} = 0.10

S_{22T} = 47.3 MPa (6,850 psi)

ε^u_{22T} = 0.0034

The tensile strength above is close to the predicted value using the maximum tensile strain criterion.

Similar coupons as above were postcured to 339°K (150°F) and then tested in tension to failure. Stress-strain curves to failure for two such coupons are shown in Figs. 18 and 19. Results obtained from five such tests are:

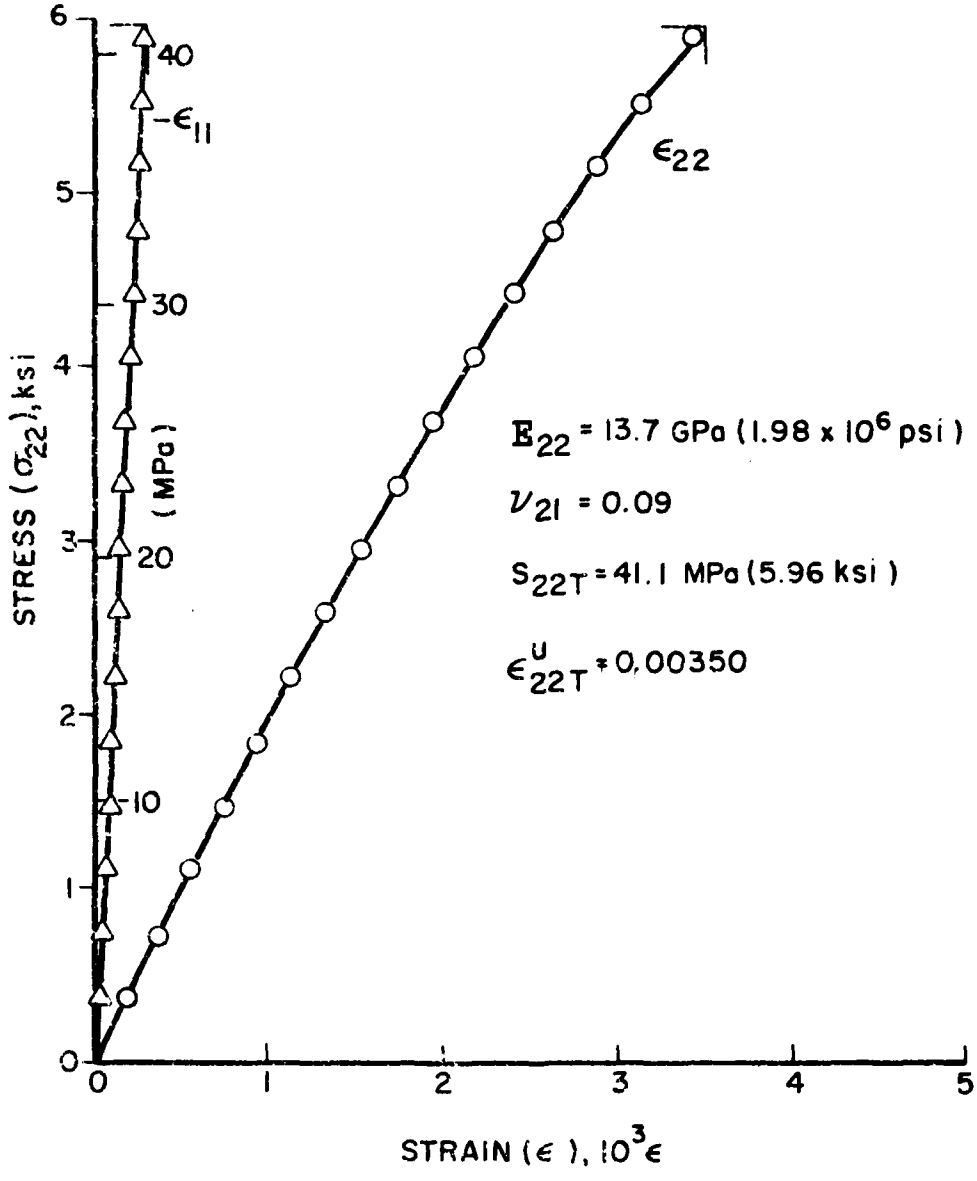

Figure 16

Stress-Strain Curves for $[90_6]$ Glass/ Epoxy Specimen Under Uniaxial Tensile Loading (Room-Temperature Cured)

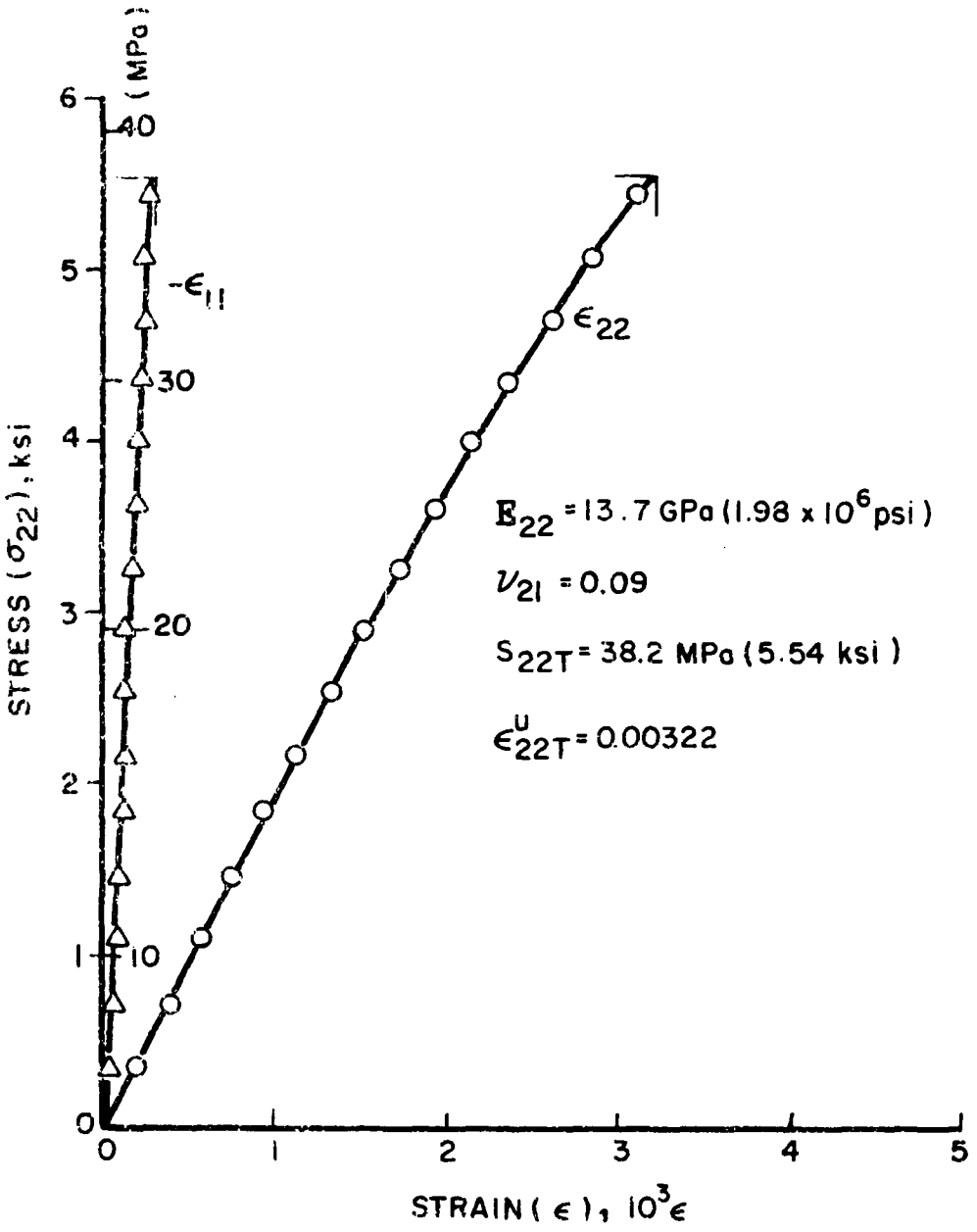

Figure 17

Stress-Strain Curves for $[90_6]$ Glass/ Epoxy Specimen Under Uniaxial Tensile Loading (Room-Temperature Cured)

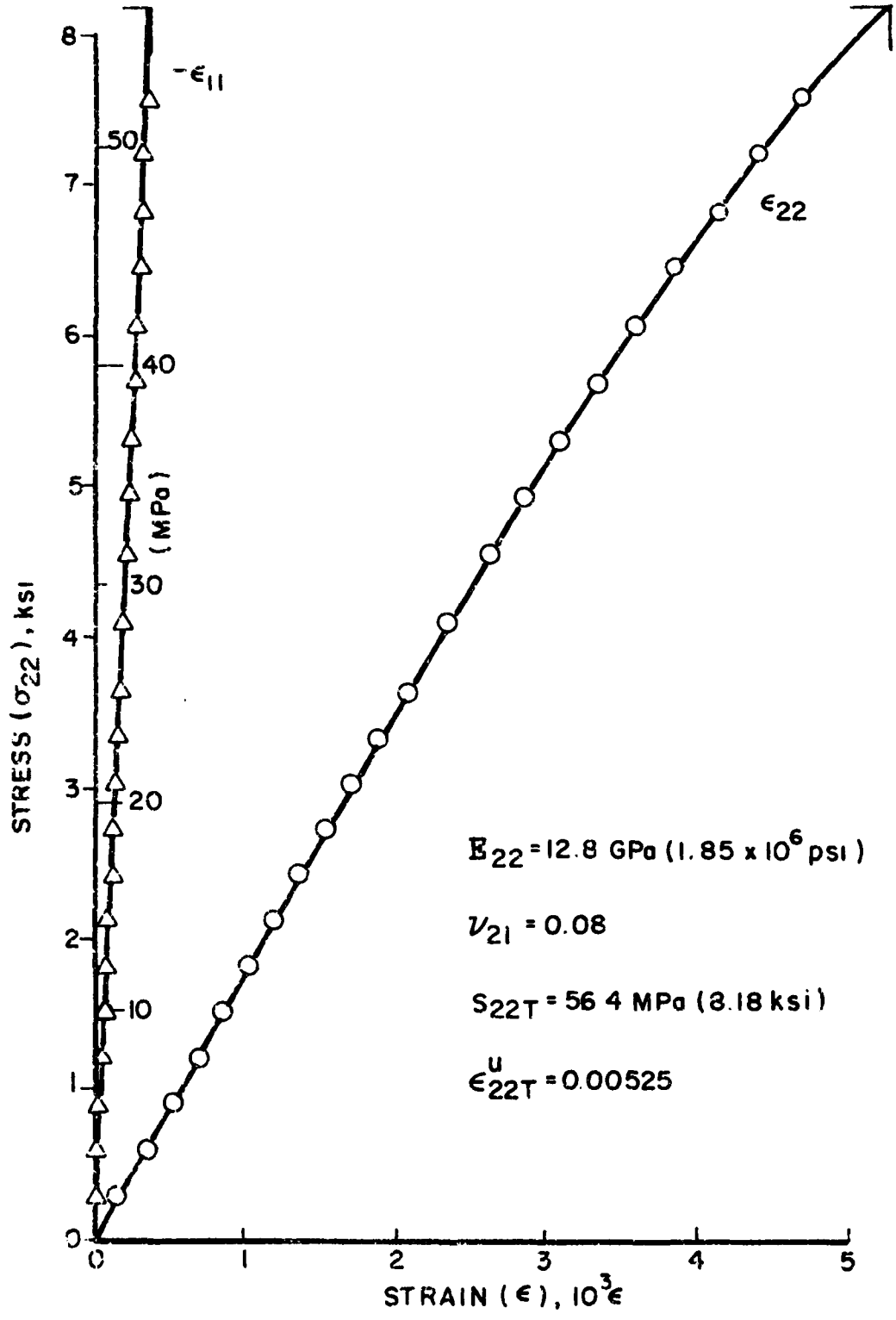

Figure 18

Stress-Strain Curves for $[90_6]$ Glass/Epoxy Specimen Under Uniaxial Tensile Loading (Post -Cured at 339°K/150°F)

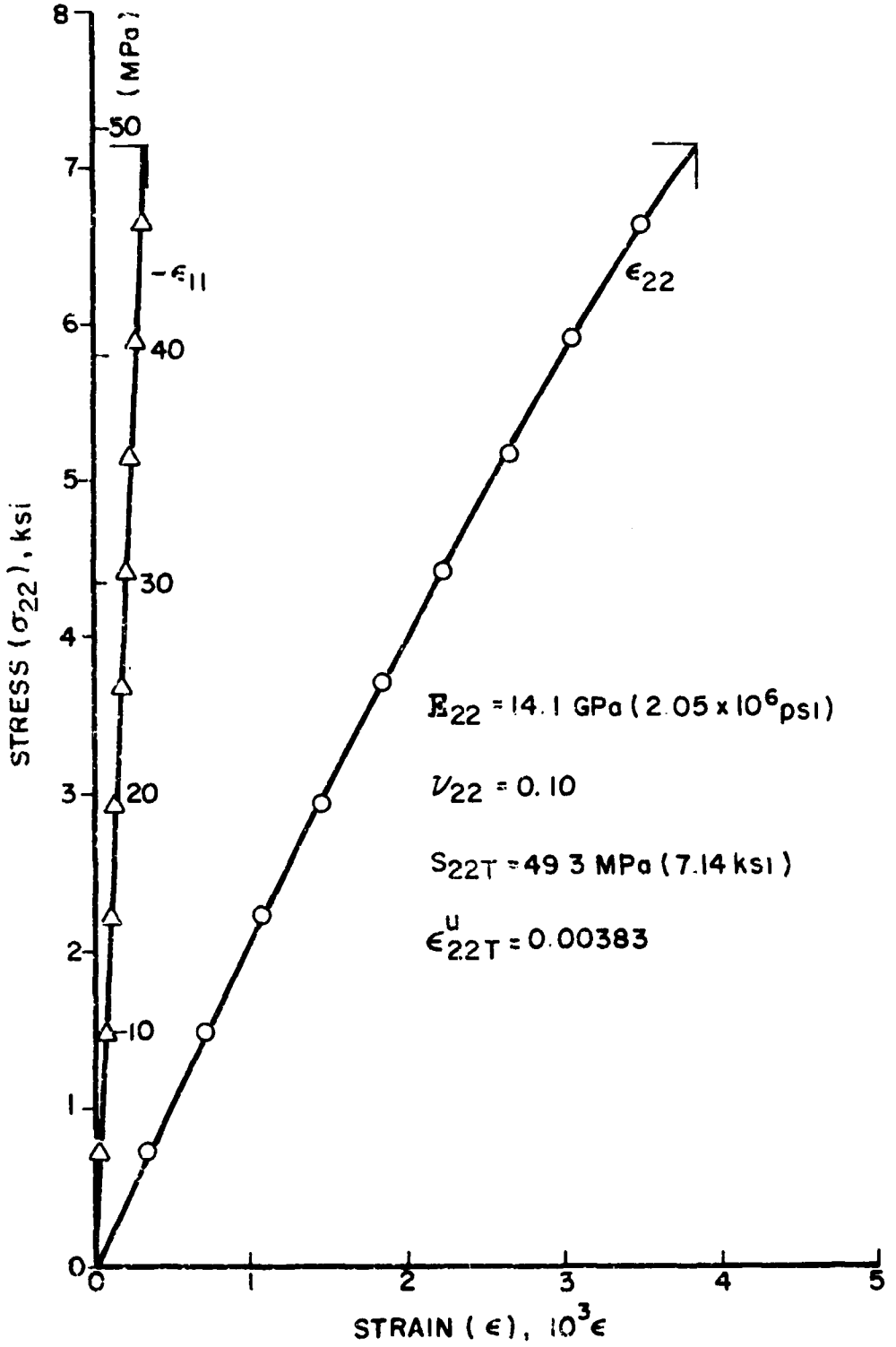

Figure 19

Stress-Strain Curves for $[90_6]$ Glass/Epoxy Specimen Under Uniaxial Tensile Loading (Post-cured at 339°K/150°F)

E_{22} = 13.5 GPa (1.95 x 10^6 psi)

ν_{21} = 0.09

S_{22T} = 56.4 MPa (8, 170 psi)

ε^u_{22T} = 0.0045

The value for the strength above is much lower than that predicted by either the maximum tensile strain or octahedral shear stress criterion.

7. SUMMARY, CONCLUSIONS AND RECOMMENDATIONS FOR FUTURE WORK

An experimental investigation was conducted using two-dimensional photoelastic models, as well as prototype composites to study internal stress distributions in unidirectional composites under transverse tensile loading. Two-dimensional photoelastic models were used to simulate the transverse cross section of a unidirectional composite with a 0.50 fiber volume ratio.

The determination of residual curing stresses was reduced to the measurement of the maximum fringe order at the interface of a single isolated inclusion in the matrix. It was found that residual stresses in the room-temperature cured matrix used increased sharply with postcuring temperature. The variation of the interface residual stress with postcuring temperature was plotted. This stress varied from 2.0 MPa (290 psi) for a room-temperature cured matrix to 7.6 MPA (1096 psi) for the same matrix postcured to 339°K (150°F).

The maximum stress at the inclusion matrix interface was determined from the photoelastic specimens. The stress concentration was determined as $k_\sigma = 1.95$ for the composite models tested. The strain concentration is much higher as it is proportional to the ratio of the composite to the matrix modulus. For the composites studied here the maximum strain concentration was determined as $k_\varepsilon = 3.81$.

The transverse tensile strength of the composite was calculated based on the determination of residual and loading stresses and using two criteria, the maximum tensile strain and octahedral shear stress criteria.

Prototype composite specimens were made with the same matrix material and the same fiber volume ratio and were cured under the same conditions as the photoelastic models. One group of specimens was cured at room temperature only and the other group was postcured to 339°K (150°F). The measured transverse tensile strength of the room-temperature cured specimens was in good agreement with that predicted by the maximum tensile strain criterion.

The octahedral shear stress criterion overestimated the transverse strength. In the case of the postcured specimens, both criteria overestimated the measured strength.

From the results above, it is seen that a better understanding of the nature of residual stresses and their effect on the strength of composites is needed. The dependence of residual stresses on the curing cycle, including cool-down path and postcure cycle should be investigated using photoelastic models. The relaxation of these stresses with time should be measured.

The failure modes in transversely loaded composites with various magnitudes of residual stress, should be studied in order to arrive at more reliable failure criteria.

Environment-induced dilational stresses (thermal and moisture stresses) and their effects on composite behavior, should be studied. Internal stress distributions should be determined for various hygrothermal/loading conditions. These studies could be conducted using photoelastic models. Predictions from these studies should be checked by testing prototype composite specimens under specific hygrothermal conditions.

REFERENCES

1. J.A. Kies, "Maximum Strains in the Resin of Fiberglass Composites," NRL Report 5752, March 1962.

2. L.R. Hermann and K.S. Pister, "Composite Properties of Filament-Resin Systems," ASME Paper No. 63-WA-239, 1963.

3. R. Hill, "Elastic Properties of Reinforced Solids : Some Theoretical Principles," J. Mech. Phys. Solids, Vol. II, p. 357, 1963.

4. Z. Hashin, "Theory of Mechanical Behavior of Heterogeneous Media," Applied Mechanics Reviews, January 1964.

5. Z. Hashin and B.W. Rosen, "The Elastic Moduli of Fiber Reinforced Materials," J. Appl. Mech., Vol. 31, p. 223, 1964.

6. R. Hill, "Theory of Mechanical Properties of Fibre-Strengthened Materials - I. Elastic Behavior," J. Mech. Phys. Solids, Vol. 12, p. 199, 1964.

7. G. Pickett and M.W. Johnson, "Analytical Procedures for Predicting the Mechanical Properties of Fiber Reinforced Composites," AFFL-TR-65-220, 1965.

8. Z. Hashin, "On Elastic Behavior of Fibre Reinforced Materials of Arbitrary Transverse Phase Geometry," J. Mech. Phys. Solids, Vol. 13, p. 119, 1965.

9. H.B. Wilson and J.L. Hill, "Plane Elastostatic Analysis of an Infinite Plate with a Doubly Periodic Array of Holes or Rigid Inclusions," in Mathematical Studies of Composite Materials II, Rohm and Haas Co., Report No. S-50, 39, 1965.

10. Z. Hashin, "Viscoelastic Fiber Reinforced Materials," AIAA Journal, Vol. 4, No. 8, pp. 1411-1417, Aug. 1966.

11. R.L. Foye, "Structural Composites," North American Aviation, Columbus Div., Contract No. AF33 (615)-5150, Quarterly Reports No. 1, 2, 3, Sept. 1966, Dec. 1966, March 1967.

12. D.F. Adams and D.R. Doner, "Transverse Normal Loading of a Unidirectional Composite," J. Composite Materials, Vol. 1, pp. 152-164, 1967.

REFERENCES (Cont'd)

13. W.F. Clausen and A.W. Leissa, "Stress and Deflection Analysis of Fibrous Composite Materials," Air Force Materials Laboratory, Wright-Patterson Air Force Base, Ohio, AFML-TR-67-151, 1967.

14. J.M. Whitney, "Elastic Moduli of Unidirectional Composites with Anisctropic Filaments," J. Composite Mateials, Vol. 1, pp. 188-193, 1967.

15. C.H. Chen and S. Cheng, "Mechanical Properties of Fiber Reinforced Composites," J. Composite Mats., Vol. 1, p. 30, 1967.

16. D.F. Adams, D.R. Doner and R.L. Thomas, "Mechanical Behavior of Fiber-Reinforced Composite Materials," AFML-TR-67-96, 1967.

17. G. Pickett, "Elastic Moduli of Fiber Reinforced Plastic Composites," in Fundamental Aspects of Fiber Reinforced Plastic Composites, R.T. Schwartz and H.S. Schwartz, Eds., Chap. 2, Interscience, 1968.

18. B.S. Shaffer, "Elastic-Plastic Stress Distribution within Reinforced Plastic Loaded Normal to its Internal Filaments," AIAA Journal, Vol. 6, No.12, pp. 2316-2324, Dec. 1968.

19. D.F. Adams and S.W. Tsai, "The Influence of Random Filament Packing on the Elastic Properties of Composite Materials," The Rand Corp., Memorandum RM-5608-PR, Dec. 1968.

20. Z. Hashin, "Analysis of Properties of Fiber Composites with Anisotropic Constituents, "J. Appl. Mech. Vol. 46. p. 543, 1979.

21. Z. Hashin, "Theory of Fiber Reinforced Mateials," NASA CR-1974, 1972.

22. R.M. Christensen, Mechanics of Composite Materials, J. Wiley, 1979.

23. I.M. Daniel and A.J. Durelli, "Photoelastic Investigation of Residual Stresses in Glass-Plastic Composites," Proc. of 16th Conf. of Reinf. Plastics Div., Soc. of Plastics Industry, Sec. 19-A, pp. 1-8, Feb. 1961.

24. I.M. Daniel and A.J. Durelli, "Shrinkage Stresses Around Rigid Inclusions," Exp. Mechanics, Vol. 2 pp. 240-244, 1962.

REFERENCES (Cont'd)

25. T. Koufopoulos and P.S. Theocaris, "Shrinkage Stresses in Two-Phase Materials," J. Composite Materials, Vol. 3, pp. 308-320, April 1969.

26. R.C. Sampson, "Photoelastic Studies of Solid Propellant Grain Stress Distribution," in "Study of Mechanical Properties of Solid Rocket Propellants," Aerojet-General Corp., Report No. 0411-10F, 1962.

27. I.M. Daniel, 'Photoelastic Studies of Mechanics of Composites," In IIT Research Institute Report No. M6132 to General Dynamics: Application of Advanced Fibrous Reinforced Composite Materials, Contract AF33 (615)-3323, July 1966.

28. I.M. Daniel, "Micromechanics" in "Structural Airframe Application of Advanced Composite Materials," Tech. Report AFML-TR-69-101. Vol. II, Sept. 1969.

29. R.H. Marloff and I.M Daniel, "Three-Dimensional Photoelastic Analysis of a Fiber-Reinforced Composite Model," Exp. Mechanics, Vol. 9, pp. 156-162, April 1969.

30. D.F. Adams, private communication, 1968.

DISTRIBUTION LIST

No. of Copies	To
1	Office of the Under Secretary of Defense for Research and Engineering, The Pentagon, Washington, D.C. 20301
12	Commander, Defense Technical Information Center, Cameron Station, Building 5, 5010 Duke Street, Alexandria, Virginia 22314
1	Metals and Ceramics Information Center, Battelle Columbus Laboratories, 505 King Avenue, Columbus, Ohio 43201
	Deputy Chief of Staff, Research, Development, and Acquisition, Headquarters, Department of the Army, Washington, D.C. 20310
1	ATTN: DAMA-ARZ
1	Dr. J. I. Bryant
	Commander, Army Research Office, P.O. Box 12211, Research Triangle Park, North Carolina 27709
1	ATTN: Information Processing Office
1	Dr. J. Hurt
1	Dr. G. Mayer
1	Dr. D. Squire
	Commander, U.S. Army Materiel Development and Readiness Command, 5001 Eisenhower Avenue, Alexandria, Virginia 22333
1	ATTN: DRCLDC
	Commander, U.S. Army Missile Command, Redstone Arsenal, Alabama 35809
1	ATTN: Mr. Donald Lovelace
	Commander, U.S. Army Armament Research and Development Command, Dover, New Jersey 07801
1	ATTN. Mr. H. Pebly, PLASTEC
1	Mr. A. Slobodzinski, PLASTEC
1	Mr. W. Tanner
	Commander, U.S. Army Natick Research and Development Command, Natick, Massachusetts 01760
1	ATTN: Technical Library
	Commander, U.S. Army Aviation Research and Development Command, 4300 Goodfellow Boulevard, St. Louis, Missouri 63120
1	ATTN: Mr. R. Vollmer
	Commander, Harry Diamond Laboratories, 2800 Powder Mill Road, Adelphi, Maryland 20783
1	ATTN. Technical Information Office

No. of Copies	To
	Commander, U.S. Army Foreign Science and Technology Center, 220 7th Street, N.E., Charlottesville, Virginia 22901
1	ATTN: Military Tech, Mr. Marley
	Director, Eustis Directorate, U.S. Army Air Mobility Research and Development Laboratory, Fort Eustis, Virginia 23604
2	ATTN: Mr. W. Figgel
	Chief of Naval Research, Arlington, Virginia 22217
1	ATTN: Code 471
	Office of Naval Research, Boston Branch, 495 Summer Street, Boston, Massachusetts 02210
1	ATTN: Dr. L. H. Peebles
	Naval Research Laboratory, Washington, D.C. 20375
1	ATTN: Dr. W. B. Moniz, Code 6120
1	Dr. I. Wolock, Code 8433
1	Dr. W. D. Bascom, Code 6170
1	Dr. L. B. Lockhart, Jr., Code 6120
	Commander, Naval Air Systems Command, Washington, D.C. 20361
2	ATTN: Mr. C. Bersch
	Commander, Naval Surface Weapons Center, White Oak, Silver Spring, Maryland 20910
1	ATTN: Dr. J. M. Augl
	Air Force Office of Scientific Research (NC), Building 410, Bolling Air Force Base, Washington, D.C. 20332
1	ATTN: Dr. D. R. Ulrich
	Air Force Materials Laboratory, Wright-Patterson Air Force Base, Ohio 45433
1	ATTN: Dr. S. W. Tsai
1	Dr. N. J. Pagano
1	Dr. H. T. Hahn
1	Dr. C. E. Browning
	Air Force Flight Dynamics Laboratory, Wright-Patterson Air Force Base, Ohio 45433
1	ATTN: Dr. G. P. Sendeckyj
	National Aeronautics and Space Administration, Lewis Research Center, 21000 Brookpark Road, Cleveland, Ohio 44135
1	ATTN: Dr. T. T. Serafini (49-1)
1	Dr. C. C. Chamis
1	Professor D. F. Adams, Department of Mechanical Engineering, University of Wyoming, Laramie, Wyoming 82070

No. of Copies	To
1	Professor F. J. McGarry, MIT, Cambridge, Massachusetts 02139
1	Professor K. H. G. Ashbee, University of Bristol, H. H. Wills Physics Lab., Bristol, England BS81TL
1	Professor O. Ishai, Department of Mechanics, Technicon - Israel Institute of Technology, Haifa, Israel
1	Dr. D. H. Kaelble, Science Center, Rockwell International, Thousand Oaks, California 91360
1	Dr. B. W. Rosen, Materials Science Corporation, Blue Bell, Pennsylvania 19422
1	Professor D. Martin, 252 E.R.I. Building, Iowa State University, Ames, Iowa 50011
1	Dr. W. J. Renton, Advanced Composites, Vought Corporation, P.O. 225907, Dallas, Texas 75265
1	Dr. C. A. Matzkanin, Southwest Research Institute, 6220 Culebra Road, San Antonio, Texas 78284
	Defense Research Establishment Office, Sheelay Bay, Ottawa, Ontario KIA 024
1	ATTN: Mr. H. L. Nash
	Defence Standard Laboratories, Department of Supply, P.O. Box 50, Ascot Vale 3032, Victoria, Australia
1	ATTN: Dr. D. Pinkerton
1	Dr. G. George
	Director, Army Materials and Mechanics Research Center, Watertown, Massachusetts 02172
2	ATTN: DRXMR-PL
1	DRXMR-PR
1	DRXMR-AP
1	DRXMR-PD
10	DRXMR-PP, Dr. A. Wilde

Army Materials and Mechanics Research Center
Watertown, Massachusetts 02172
PHOTOELASTIC STUDIES OF INTERNAL
STRESS DISTRIBUTIONS OF UNIDIRECTIONAL
COMPOSITES
I. M. Daniel, G. M. Koller, T. Niiro
IIT Research Institute, 10 W. 35th Street
Chicago, Ill. 60616
Technical Report AMMRC TR 80-56, December 1980, 42 pp.
illus. Contract DAAG46-79-C-0083
D/A Project 1L161102AH42, AMCMS Code 611O2 11 H42
Final Report, 11 September 1979 to 11 September 1980

AD _____
Unclassified
Unlimited Distributions

Key Words
Composite materials
Micromechanics
Glass/epoxy composites
Stress concentration
Residual stresses
Failure
Failure criteria

Two-dimensional photoelastic models were used to determine internal loading- and residual-stress distributions on the transverse cross section of unidirectional composites. The variation of residual stress was determined as a function of post-curing temperature for a room-temperature cured matrix resin. Maximum stresses and strains were determined in the matrix of a unidirectional composite with a 0.50 fiber volume ratio. Prototype composite specimens were made with the same matrix material and the same fiber volume ratio and were cured under the same conditions as the models. The transverse strength of these prototype specimens was predicted satisfactorily from results of model tests for the room-temperature cured specimens. In the case of the post-cured specimens, the predicitons were higher than the measured strength.

Army Materials and Mechanics Research Center
Watertown, Massachusetts 02172
PHOTOELASTIC STUDIES OF INTERNAL
STRESS DISTRIBUTIONS OF UNIDIRECTIONAL
COMPOSITES
I. M. Daniel, G. M. Koller, T. Niiro
IIT Research Institute, 10 W. 35th Street
Chicago, Ill. 60616
Technical Report AMMRC TR 80-56, December 1980, 42 pp.
illus. Contract DAAG46-79-C-0083
D/A Project 1L161102AH42, AMCMS Code 611O2 11 H42
Final Report, 11 September 1979 to 11 September 1980

AD _____
Unclassified
Unlimited Distributions

Key Words
Composite materials
Micromechanics
Glass/epoxy composites
Stress concentration
Residual stresses
Failure
Failure criteria

Two-dimensional photoelastic models were used to determine internal loading- and residual-stress distributions on the transverse cross section of unidirectional composites. The variation of residual stress was determined as a function of post-curing temperature for a room-temperature cured matrix resin. Maximum stresses and strains were determined in the matrix of a unidirectional composite with a 0.50 fiber volume ratio. Prototype composite specimens were made with the same matrix material and the same fiber volume ratio and were cured under the same conditions as the models. The transverse strength of these prototype specimens was predicted satisfactorily from results of model tests for the room-temperature cured specimens. In the case of the post-cured specimens, the predicitons were higher than the measured strength.

Army Materials and Mechanics Research Center
Watertown, Massachusetts 02172
PHOTOELASTIC STUDIES OF INTERNAL STRESS DISTRIBUTIONS OF UNIDIRECTIONAL COMPOSITES
I. M. Daniel, G. M. Koller, T. Niiro
IIT Research Institute, 10 W. 35th Street
Chicago, IL 60616
Technical Report AMMRC TR 80-56, December 1980, 42 pp-illus. Contract DAAG46-79-C-0083
D/A Project 1L161102AH42, AMCMS Code: 611102.11.H42
Final Report, 11 September 1979 to 11 September 1980

AD ________ Unclassified
Unlimited Distributions

Key Words

Composite materials
Micromechanics
Glass/epoxy composites
Stress concentration
Residual stresses
Failure
Failure criteria

Two-dimensional photoelastic models were used to determine internal loading- and residual-stress distributions on the transverse cross section of unidirectional composites. The variation of residual stress was determined as a function of post-curing temperature for a room-temperature cured matrix resin. Maximum stresses and strains were determined in the matrix of a unidirectional composite with a 0.50 fiber volume ratio. Prototype composite specimens were made with the same matrix material and the same fiber volume ratio and were cured under the same conditions as the models. The transverse strength of these prototype specimens was predicted satisfactorily from results of model tests for the room-temperature cured specimens. In the case of the post-cured specimens, the predicitons were higher than the measured strength.

Army Materials and Mechanics Research Center
Watertown, Massachusetts 02172
PHOTOELASTIC STUDIES OF INTERNAL STRESS DISTRIBUTIONS OF UNIDIRECTIONAL COMPOSITES
I. M. Daniel, G. M. Koller, T. Niiro
IIT Research Institute, 10 W. 35th Street
Chicago, IL 60616
Technical Report AMMRC TR 80-56, December 1980, 42 pp-illus. Contract DAAG46-79-C-0083
D/A Project 1L161102AH42, AMCMS Code: 611102.11.H42
Final Report, 11 September 1979 to 11 September 1980

AD ________ Unclassified
Unlimited Distributions

Key Words

Composite materials
Micromechanics
Glass/epoxy composites
Stress concentration
Residual stresses
Failure
Failure criteria

Two-dimensional photoelastic models were used to determine internal loading- and residual-stress distributions on the transverse cross section of unidirectional composites. The variation of residual stress was determined as a function of post-curing temperature for a room-temperature cured matrix resin. Maximum stresses and strains were determined in the matrix of a unidirectional composite with a 0.50 fiber volume ratio. Prototype composite specimens were made with the same matrix material and the same fiber volume ratio and were cured under the same conditions as the models. The transverse strength of these prototype specimens was predicted satisfactorily from results of model tests for the room-temperature cured specimens. In the case of the post-cured specimens, the predicitons were higher than the measured strength.

Army Materials and Mechanics Research Center
Watertown, Massachusetts 02172
PHOTOELASTIC STUDIES OF INTERNAL STRESS DISTRIBUTIONS OF UNIDIRECTIONAL COMPOSITES
I. M. Daniel, G. M. Koller, T. Niiro
IIT Research Institute, 10 W. 35th Street
Chicago, IL 60616
Technical Report AMMRC TR 80-56, December 1980, 42 pp-illus. Contract DAAG46-79-C-0083
D/A Project 1L161102AH42, AMCMS Code: 611102.11.H42
Final Report, 11 September 1979 to 11 September 1980

AD ________ Unclassified
Unlimited Distributions

Key Words

Composite materials
Micromechanics
Glass/epoxy composites
Stress concentration
Residual stresses
Failure
Failure criteria

Two-dimensional photoelastic models were used to determine internal loading- and residual-stress distributions on the transverse cross section of unidirectional composites. The variation of residual stress was determined as a function of post-curing temperature for a room-temperature cured matrix resin. Maximum stresses and strains were determined in the matrix of a unidirectional composite with a 0.50 fiber volume ratio. Prototype composite specimens were made with the same matrix material and the same fiber volume ratio and were cured under the same conditions as the models. The transverse strength of these prototype specimens was predicted satisfactorily from results of model tests for the room-temperature cured specimens. In the case of the post-cured specimens, the predicitons were higher than the measured strength.

Army Materials and Mechanics Research Center
Watertown, Massachusetts 02172
PHOTOELASTIC STUDIES OF INTERNAL STRESS DISTRIBUTIONS OF UNIDIRECTIONAL COMPOSITES
I. M. Daniel, G. M. Koller, T. Niiro
IIT Research Institute, 10 W. 35th Street
Chicago, IL 60616
Technical Report AMMRC TR 80-56, December 1980, 42 pp-illus. Contract DAAG46-79-C-0083
D/A Project 1L161102AH42, AMCMS Code: 611102.11.H42
Final Report, 11 September 1979 to 11 September 1980

AD ________ Unclassified
Unlimited Distributions

Key Words

Composite materials
Micromechanics
Glass/epoxy composites
Stress concentration
Residual stresses
Failure
Failure criteria

Two-dimensional photoelastic models were used to determine internal loading- and residual-stress distributions on the transverse cross section of unidirectional composites. The variation of residual stress was determined as a function of post-curing temperature for a room-temperature cured matrix resin. Maximum stresses and strains were determined in the matrix of a unidirectional composite with a 0.50 fiber volume ratio. Prototype composite specimens were made with the same matrix material and the same fiber volume ratio and were cured under the same conditions as the models. The transverse strength of these prototype specimens was predicted satisfactorily from results of model tests for the room-temperature cured specimens. In the case of the post-cured specimens, the predicitons were higher than the measured strength.

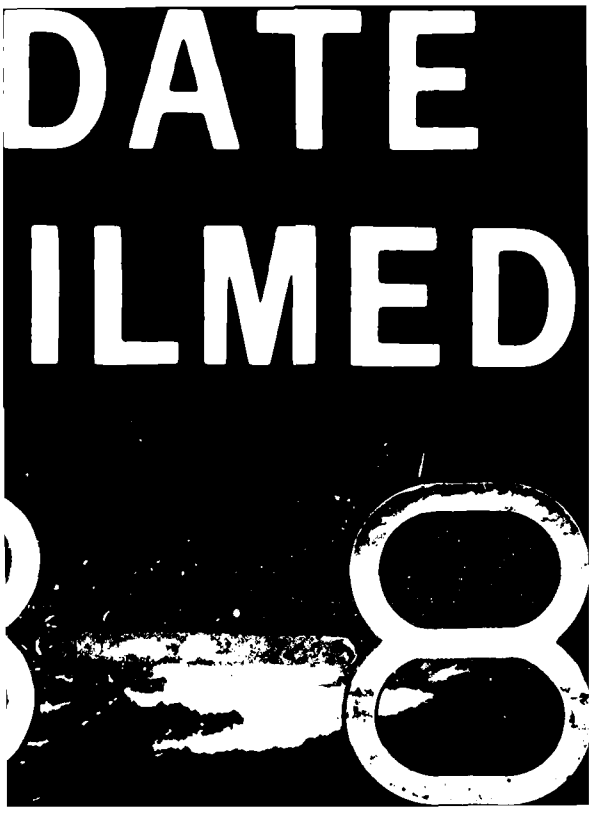
DATE
ILMED